Marine Pollution Bulletin 135 (2018) 427–440

Contents lists available at ScienceDirect

Marine Pollution Bulletin

journal homepage: www.elsevier.com/locate/marpolbul

Degradation of petroleum hydrocarbons in seawater by simulated surface-level atmospheric ozone: Reaction kinetics and effect of oil dispersant

Haodong Ji[a], Yanyan Gong[a,b], Jun Duan[a], Dongye Zhao[c,a,*], Wen Liu[a,d,**]

[a] Environmental Engineering Program, Department of Civil Engineering, Auburn University, Auburn, AL 36849, USA
[b] School of Environment, Guangzhou Key Laboratory of Environmental Exposure and Health, Guangdong Key Laboratory of Environmental Pollution and Health, Jinan University, Guangzhou 510632, China
[c] College of Environment and Energy, Beijing University of Civil Engineering and Architecture, Beijing 100044, China
[d] The Key Laboratory of Water and Sediment Science, Ministry of Education, College of Environment Science and Engineering, Peking University, Beijing 100871, China

ARTICLE INFO

Keywords:
Atmospheric ozone
Ozonation
Oil spill
Oil dispersant
Oil weathering
Petroleum hydrocarbon

ABSTRACT

Oil degradation by surface-level atmospheric ozone has been largely ignored in the field. To address this knowledge gap, this study investigated the ozonation rate and extent of typical petroleum compounds by simulated surface-level ozone, including total petroleum hydrocarbons (TPHs), *n*-alkanes, and polycyclic aromatic hydrocarbons (PAHs). Moreover, the work explored the effect of a prototype oil dispersant, Corexit EC9500A, on the ozonation rate. Rapid oxidation of TPHs, *n*-alkanes and PAHs was observed at various gaseous ozone concentrations (i.e. 86, 200 and 300 ppbv). Generally, the presence of the oil dispersant enhanced ozonation of the oil compounds. The addition of humic acid inhibited the reaction, while increasing salinity accelerated the degradation. Both direct ozonation by molecular ozone and indirect oxidation by ozone-induced radicals play important roles in the degradation process. The findings indicate that ozonation should be taken into account in assessing environmental fate and weathering of spilled oil.

1. Introduction

The 2010 Deepwater Horizon (*DwH*) oil spill released > 795 million L of Louisiana Sweet Crude (LSC) oil into the Gulf of Mexico (Camilli et al., 2010; Reddy et al., 2012; Sammarco et al., 2013). As a result, high concentrations of oil compounds in the water column were detected following the spill. For instance, Camilli et al. (2010) reported that the concentration of mono-aromatic petroleum hydrocarbons in the affected seawater exceeded 50 mg/L, and Reddy et al. (2012) observed that the light aromatic hydrocarbons (benzene, toluene, ethylbenzene, and total xylenes) reached up to 78 mg/L. The *DwH* oil contained ~3.9% total polycyclic aromatic hydrocarbons (TPAHs), ~1.5% alkylated PAHs, and ~15.3% *n*-alkanes by weight; as such, the incident released approximately ~2.1×10^7 kg of TPAHs, ~7.9×10^6 kg of alkylated PAHs, and ~8.1×10^7 kg of *n*-alkanes into the Gulf of Mexico (Reddy et al., 2012).

As an emergency mitigation measure, two chemical dispersants, Corexit EC9500A (6.8 million L) and Corexit EC9527A (1.1 million L) were applied at the wellhead and on the seawater surface to disperse the oil slicks into the water column (Kujawinski et al., 2011). As a result, it was estimated that 16% of the spilled oil was dispersed by chemical dispersants (Ramseur, 2010). While several recent studies have reported that oil dispersant enhanced degradation of oil, particularly *n*-alkanes, under conditions relevant to the northern Gulf of Mexico, a thorough understanding of the process and mechanisms is needed (Bacosa et al., 2015; Liu et al., 2016).

A number of physical, chemical and biological processes can affect the fate and transport of spilled oil, including spreading, drifting, evaporation and dissolution (Liu et al., 2012, 2017; Ryerson et al., 2011), dispersion of oil droplets into the water column (Conmy et al., 2014; Kleindienst et al., 2015), interactions of dissolved and dispersed oil compounds with suspended particulate matter and sediment particles (Fu et al., 2014; Gong et al., 2014; Zhao et al., 2015; Zhao et al., 2016), sorption (Gong et al., 2014; Zhao et al., 2015; Zhao et al., 2016), bioaccumulation and biodegradation (Baumard et al., 1998), and photodegradation (Gong et al., 2015; Zhao et al., 2016). Another potentially significant oil weathering process is oxidation by atmospheric ozone (O_3). However, ozonation has been completely ignored in

* Correspondence to: D. Zhao, Environmental Engineering Program, Department of Civil Engineering, Auburn University, Auburn, AL 36849, USA.
** Correspondence to: W. Liu, The Key Laboratory of Water and Sediment Science, Ministry of Education, College of Environment Science and Engineering, Peking University, Beijing 100871, China.
E-mail addresses: zhaodon@auburn.edu (D. Zhao), wen.liu@pku.edu.cn (W. Liu).

https://doi.org/10.1016/j.marpolbul.2018.07.047
Received 16 February 2018; Received in revised form 4 July 2018; Accepted 17 July 2018
Available online 23 July 2018
0025-326X/

estimating oil budget and in assessing the fate and weathering of spilled oil despite the known high reactivity and fairly high concentrations of atmospheric ozone at the ground or sea level.

Typically, surface-level ozone is formed through photochemical reactions involving volatile organic compounds (VOCs) and nitrogen oxides (Haagen-Smit et al., 1953). High levels of ozone have been widely detected at the ground level along the Gulf of Mexico coast. For instance, based on 2002–2013 monitoring data, the 8-hour average ozone in Alabama air ranged from 60 to 92 ppbv (ADEM, 2016). Nationally, the average of the fourth highest daily maximum 8-h ozone level had consistently exceeded the National Ambient Air Quality Standards (NAAQS) of 75 ppbv from 1986 through 2016 (EPA, 2017). It is noted that the ozone levels over an oil slick may be much higher than in the bulk air due to the extensive evaporation of volatile hydrocarbons from the oil slick (Ryerson et al., 2011).

Ozone is a well-known strong oxidant ($E^0 = +2.07$ V) and relatively strong electrophile (Yu et al., 2007). In engineered processes, ozone has been widely used to degrade various organic compounds, including PAHs (Chelme-Ayala et al., 2011; Lin et al., 2014; von Gunten, 2003) and *n*-alkanes (Masten and Davies, 1994; von Gunten, 2003; Yu et al., 2007). In general, ozonation of organic compounds (e.g., *n*-alkanes and PAHs) can take place in the following fashions: 1) direct attack by molecular O_3 on the σ-bond between C and H atoms via 1,3-dipolar insertion for alkanes or via cycloaddition or electrophilic reactions for PAHs (Hellman and Hamilton, 1974); and 2) indirect attack by free radicals (primarily hydroxyl radicals, ·OH) (Masten and Davies, 1994; Zhao et al., 2004, 2011). Therefore, it is reasonable to postulate that oxidation under atmospheric ozone is an important natural weathering process for petroleum hydrocarbons.

Oil dispersants are complex mixtures of anionic, nonionic surfactants, and solvents (Board and Council, 1989; Gong et al., 2014). Corexit EC9500A consists of three nonionic surfactants including ethoxylated sorbitan mono- and trioleates and sorbitan monooleate (commercially known as Tween 80, Tween 85, and Span 80) and an anionic surfactant, namely, sodium dioctyl sulfosuccinate (SDSS) and solvents as a mixture of di(propylene glycol) butyl ether (DPnB), propylene glycol, and hydro-treated light distillates (petroleum) (Cai et al., 2016; Place et al., 2010; Scelfo and Tjeerdema, 1991).

Ozonation of organic contaminants can be affected by surfactants, and the effect depends on the type of the surfactants (anionic, nonionic and cationic). Pryor and Wu (1992) reported that the ozonation of methyl oleate was increased by 1.2 times when an anionic surfactant, sodium dodecyl sulfate (SDS), was increased from 0.02 M to 0.5 M. Chiu et al. (2007) observed that the presence of a nonionic surfactant Brij 30 decreased the gas–liquid mass transfer rates of both naphthalene and ozone, resulting in reduced removal efficiency of naphthalene. Chu et al. (2006) reported that ozonation of atrazine was enhanced by 17% by adding a nonionic surfactant, Brij 35, and the researchers stated that the surfactant played dual roles in the ozonation of atrazine: 1) it increased dissolution of ozone, and 2) it served as a radical booster and hydrogen source. Therefore, oil dispersants may also affect oil ozonation. Gong and Zhao (2017) observed that the presence of 18 and 180 mg/L of Corexit EC9500A inhibited the ozonation rate of phenanthrene by 32%–80%, and that for pyrene by 51%–85%, due to competition for the reactive ozone and free radicals. They also reported that in the presence of 18 mg/L of the dispersant, the pyrene degradation rate decreased with increasing solution pH and temperature. However, information has been lacking on the effects of oil dispersants on the ozonation of petroleum hydrocarbons (e.g. TPHs, *n*-alkanes and PAHs). Moreover, the influences of ozone concentration, pH, DOM and salinity on ozonation of petroleum hydrocarbons in the presence of oil dispersants have not yet been explored.

The overall goal of this study was to investigate the ozonation rate and extent of dispersed oil in dispersant-oil-seawater systems that are exposed to relatively high surface-level atmospheric ozone, and understand the roles of a model dispersant (Corexit EC9500A) in the ozonation process. The specific objectives were to: 1) determine the ozonation rate and extent of various key petroleum components (TPHs, *n*-alkanes and PAHs) under simulated surface-level atmospheric ozone, 2) investigate effect of Corexit EC9500A on the ozone oxidation; and 3) elucidate the ozonation mechanisms. The findings will improve our understanding of the role of atmospheric ozone in the weathering of spilled oil.

2. Materials and methods

2.1. Materials

All chemicals used in this study were of analytical grade or higher unless indicated otherwise. Methanol was purchased from Alfa Aesar (Ward Hill, MA, USA). Chromatographic hexane, dichloromethane (DCM), NaOH and NaCl were obtained from Fisher Scientific (Fair lawn, NJ, USA). HCl was acquired from BDH Aristar (West Chester, PA, USA). 4-chlorobenzoic acid (*p*CBA) was procured from Acros Organics (Morris Plains, NJ, USA). A standard leonardite humic acid (LHA, IHSS 1S104H, 64% as total organic carbon (TOC)) was purchased from the International Humic Substances Society. The following standard reagents were purchased from Supelco (Bellefone, PA, USA): a standard of *n*-alkanes mixtures (C9-C40), a standard for the 16 USEPA listed PAHs (Table S1 in Supplementary Materials (SM)), two internal standards (5α-androstane for *n*-alkanes and fluorene-d_{10} for PAHs), and a surrogate standard of naphthalene-d_8, acenaphthene-d_{10}, phenanthrene-d_{10}, and benzo(*a*)pyrene-d_{12}. Corexit EC9500A was obtained by courtesy of Nalco Company (Naperville, IL, USA). Table S2 in SM gives the formulations of Corexit EC9500A.

Seawater was collected from the top 30 cm of the water column from Grand Bay, AL, USA (N30.37926/W88.30684). Before use, the sample was first passed through 0.45 μm membrane filters to remove suspended solids, and then sterilized at 121 °C for 35 min via autoclaving. Salient properties of the seawater sample are: pH = 8.1, DOM = 2.2 mg/L as TOC, salinity = 2 wt%, Cl^- = 18.55 g/L, NO_3^- = 2.55 g/L, SO_4^{2-} = 4.25 g/L, and ionic strength (IS) = 0.7 M.

A surrogate LSC oil was obtained through courtesy of BP (Houston, TX, USA). According to the supplier, the physical, chemical and toxicological properties of the surrogate oil are analogous to those of the Macondo Well crude oil of Mississippi Canyon Block 252. Before use, the crude oil was artificially weathered according to the evaporation method by Sorial et al. (2004). Briefly, 1.0 L of the crude oil was purged in the dark through a glass tube from the bottom of a flask at a constant air flowrate of ~2 L/min to remove the lighter compounds. After 10 days of the weathering process, the oil mass diminished from 807.1 to 608.5 g (by 24.6 wt%), and the density increased from 0.807 to 0.834 g/cm^3. This procedure simulates the loss of the volatile oil compounds at sea surface shortly following an oil spill (Li et al., 2009).

2.2. Experimental set-up

Fig. 1 displays the schematic of the ozonation experiment set-up. The experiments were carried out in a glass cylinder batch reactor (H × D = 5 cm × 8 cm) with a thin quartz cover. The two ports connected with Teflon tubes were for gas flow and the other two ports sealed by ground glass joints were used for sample collection. Ozone was generated from medical grade oxygen using an A2Z Ozone Generator (Model HB5735B, A2Z Ozone Inc., Louisville, Kentucky, USA), which is able to generate a maximum of 1 g ozone h^{-1}. The gas (O_2 + O_3) flow rate into the reactor was 4 mL/min controlled by an Aalborg mass flow controller (Model GFC17, Orangeburg, New York, USA). The inlet ozone-laden gas was gently passed through the surface of the reaction solution. The inlet gas-phase ozone concentration was kept at 86 ppbv, which was analyzed by a M106-L Ozone Monitor (2B Technologies, Inc., Boulder, CO, USA) through measuring the UV absorbance at 254 nm. In the outlet gas-phase, the excess ozone was

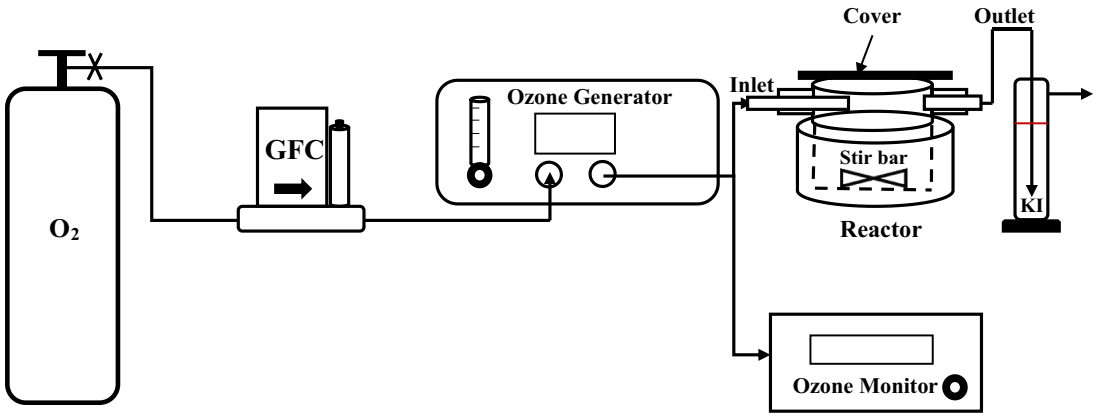

Fig. 1. Schematic of the experimental set-up for ozonation of dispersed oil under simulated atmospheric ozone. Note: GFC: gas flow controller.

passed into a gas absorption bottle containing 300 mL of a 2 wt% KI solution. All connecting tubes were Teflon-made.

2.3. Ozonation of dispersed oil and effects of dispersant

Water accommodated oil (WAO) and dispersant-facilitated water accommodated oil (DWAO) were prepared with the surrogate oil following a slightly modified protocol by Singer et al. (2000). Briefly, WAO was prepared in a 2200 mL glass aspirator bottle containing a hose bib fitted with silicon tubing and a clamp at the bottom of the vessel. About 1760 mL of the seawater was added into the bottle, leaving a ~20% headspace. Afterwards, 8.8 mL of the weathered LSC oil was added to the seawater by a glass syringe (i.e., oil-to-seawater volume ratio = 1:200). Then, the mixture was sealed and magnetically stirred for 18 h in the dark. The stirring rate was adjusted so as to obtain a vortex of ~25% of the total volume of seawater. After gravity-settling for 6 h, the WAO fraction was collected in glass vials with Teflon-lined caps from the bottom without disturbing the surface oil slicks, allowing for no headspace in the vials. The dispersed oil was prepared in the form of DWAO following the same protocol except that a dispersant solution of Corexit EC9500A was added at a dispersant-to-oil volume ratio of 1:20 (Gong et al., 2014; Zhao et al., 2016).

Batch ozonation kinetic tests were conducted in the glass cylinder reactor. For each test, the reactor was filled with 250 mL of a WAO or DWAO solution, and stirred gently (400 rpm) with a magnetic stirrer to simulate ocean wave action, which is expected to enhance the ozonation due to increased gas-water interface and mass transfer rates. The ozone-laden gas stream was then gently passed through the surface of the solution (i.e., the headspace of the reactor). At pre-determined times, each 80 mL of the solution was sampled and then analyzed for the remaining petroleum hydrocarbons (including *n*-alkanes, parent PAHs and their alkylated homologs). Control tests were carried out with nitrogen gas (no O_3) at the same gas flowrate to determine the loss of TPHs in WAO and DWAO due to volatilization. All experiments were conducted in duplicate.

To investigate effects of the dispersant, additional Corexit EC9500A (18 or 24 mg/L) was added into the as-prepared DWAO solution in selected cases, and the ozonation rates were then tested following the same kinetic experiments.

To examine the relative contributions of direct ozone oxidation and indirect oxidation (by ·OH), the ozonation kinetic tests were carried out in the presence of 3 μM of *para*-chlorobenzoic acid (*p*CBA), which has been known to be very slow in direct reaction with ozone but fast with ·OH ($k_{\cdot OH,\ pCBA} = 5 \times 10^9\ M^{-1}\ s^{-1}$, $k_{O3,\ pCBA} \leq 0.5\ M^{-1}\ s^{-1}$) (Elovitz and von Gunten, 1999).

As a control, dispersant solutions without oil were prepared under otherwise identical conditions and then analyzed for the non-petroleum hydrocarbons (i.e., hydrocarbons from the dispersant) following the procedure described in Section 2.5. The chromatographic peak areas associated with the non-petroleum hydrocarbons were deducted from those for DWAO in quantifying the petroleum hydrocarbons following the approach by Hemmer et al. (2011).

2.4. Effects of gaseous ozone concentration and solution chemistry on ozonation of petroleum hydrocarbons in DWAO

Effects of gaseous ozone concentration, pH, DOM and salinity on ozonation of petroleum hydrocarbons in DWAO were examined through the same kinetic tests as described above. To investigate the ozone concentration effect, the gaseous ozone concentration was varied from 86 to 300 ppbv, which corresponded to an aqueous ozone concentration ranging from 0.05 to 0.12 mg/L. To study the pH effect, the initial DWAO solution pH was adjusted to 6, 7, and 9 using dilute HCl (0.1 M) or NaOH (0.1 M). To examine the effect of DOM, standard leonardite humic acid was added in DWAO at 0.5, 1.0, and 5.0 mg/L as TOC. To test the effect of salinity, the initial solution salinity was varied from 2 to 8 wt% by adding a NaCl stock solution (25 wt%).

2.5. Analytical methods

Oil concentrations in WAO or DWAO were quantified based on analysis of TPHs, *n*-alkanes, and PAHs. During the kinetic tests, each 80 mL of the solution sample was extracted with dichloromethane (DCM) in three consecutive steps (5 mL DCM in each step) according to EPA Method 3510C (EPA, 1996), and then the extracts were combined and filtered through a glass column (L × D = 3 × 1 cm) packed with 5 g of anhydrous sodium sulfate to remove moisture, and then concentrated to 4 mL under a gentle nitrogen flow. Then, the concentrated samples were filtered through a polytetrafluoroethylene (PTFE) membrane (0.22 μm) filter, and split into two even subsamples in two amber glass vials (2 mL each and labeled as B1 and B2). Then, the B1 fraction was analyzed for *n*-alkanes and PAHs by gas chromatography/mass spectrometry (GC–MS) (Agilent 7890A GC coupled with the 5975C Series mass spectrometry, Agilent Technologies Inc., Santa Clara, CA, USA) equipped with a DB-EUPAH column (30 m × 0.18 mm, 0.14 μm film thickness) following the method described in Section 1 in SM. Sixteen parent PAHs (Table S1 in SM) (specified in EPA Method 610 (EPA, 1984)) and *n*-alkanes (C9-C40) were targeted. The B2 subsample was analyzed for TPHs following the method described in Section 1 of SM using gas chromatograph with a flame ionization detector (GC-FID, Agilent 6890 GC-FID) equipped with a DB5 column.

The *p*CBA concentration in the aqueous phase was analyzed via high performance liquid chromatography (HPLC, Agilent Technologies, 1260 Infinity, DE, USA) with a UV detector and at a wavelength of 240 nm. A Poroshell 120 EC-C18 column (50 × 4.6 mm, 2.7 μm) was used, with the oven temperature held constant at 30 °C. An eluent

consisting of 60%:40% (v:v) of methanol:H_2O (adjusted to pH 2 using H_3PO_4) was used as the mobile phase and the flowrate was 1 mL/ min (Rosenfeldt et al., 2006).

Dissolved ozone concentration was measured within 1 min after sampling on a UV–vis spectrophotometer (SpectraMax M2, Molecular Devices, CA, USA) at a wavelength of 258 nm shown in Fig. S1 in SM (Bader and Hoigné, 1981; Fujita et al., 2004), which gives a detection limit of 0.01 mg/L.

3. Results and discussion

3.1. Effects of oil dispersant on volatilization and ozonation of petroleum hydrocarbons in seawater

Volatilization is a parallel process along with the ozonation reactions of various oil components. Therefore, an integrated pseudo first-order kinetic model was employed to interpret the overall dissipation rates of TPHs, *n*-alkanes and total PAHs (Lin et al., 2014; Ning et al., 2015):

$$\ln(C_t/C_0) = -kt = -(k_v + k_o)t \quad (1)$$

where C_0 (mg/L) and C_t (mg/L) are the reactant concentrations at time $t = 0$ and t (h), respectively; k (h^{-1}) and k_v (h^{-1}) are the pseudo first-order rate constants of overall depletion and volatilization, respectively; and k_o (h^{-1}) is the ozonation rate constant. The values of k and k_v were obtained by fitting Eq. (1) to the corresponding experimental kinetic data (ozonation and volatilization control tests), and k_o was then calculated from the difference.

Fig. 2 shows the volatilization and ozonation kinetics of TPHs (Fig. 2a), *n*-alkanes (Fig. 2b) and PAHs (Fig. 2c) under a simulated atmospheric ozone level of 86 ppbv. The initial concentration of TPHs, *n*-alkanes and total PAHs were 0.79, 0.12 and 0.52 mg/L, respectively, in WAO, which were raised to 149.7, 79.1 and 6.2 mg/L in DWAO. Evidently, the presence the dispersant (238 mg/L) increased the concentrations of TPHs by 189 times, *n*-alkanes by 648 times and total PAHs by 12 times compared to those in WAO, which also indicates that the dispersant is more effective for dispersing *n*-alkanes than PAHs. Control tests with nitrogen gas indicated that volatilization losses of TPHs, *n*-alkanes, and total PAHs were 15.8%, 14.8% and 20.5% in WAO in 48 h, respectively, and the percentiles rose to 56.7%, 36.9% and 52.1% in DWAO, indicating that a larger fraction of the dispersed oil components is volatile than the truly dissolve counterparts. When exposed to the gaseous ozone, the overall depletion of TPHs, *n*-alkanes, and total PAHs were 56.7%, 98.9% and 81.0% in WAO, and 88.7%, 98.7% and 89.6% in DWAO, respectively, indicating that the ozonation was very reactive in degrading high concentrations of oil hydrocarbons in the dispersant solution.

Table 1 gives the model-fitted kinetic parameters for volatilization and ozonation of TPHs, *n*-alkanes and total PAHs in WAO and DWAO. Both volatilization and overall dissipation of TPHs, *n*-alkanes and total

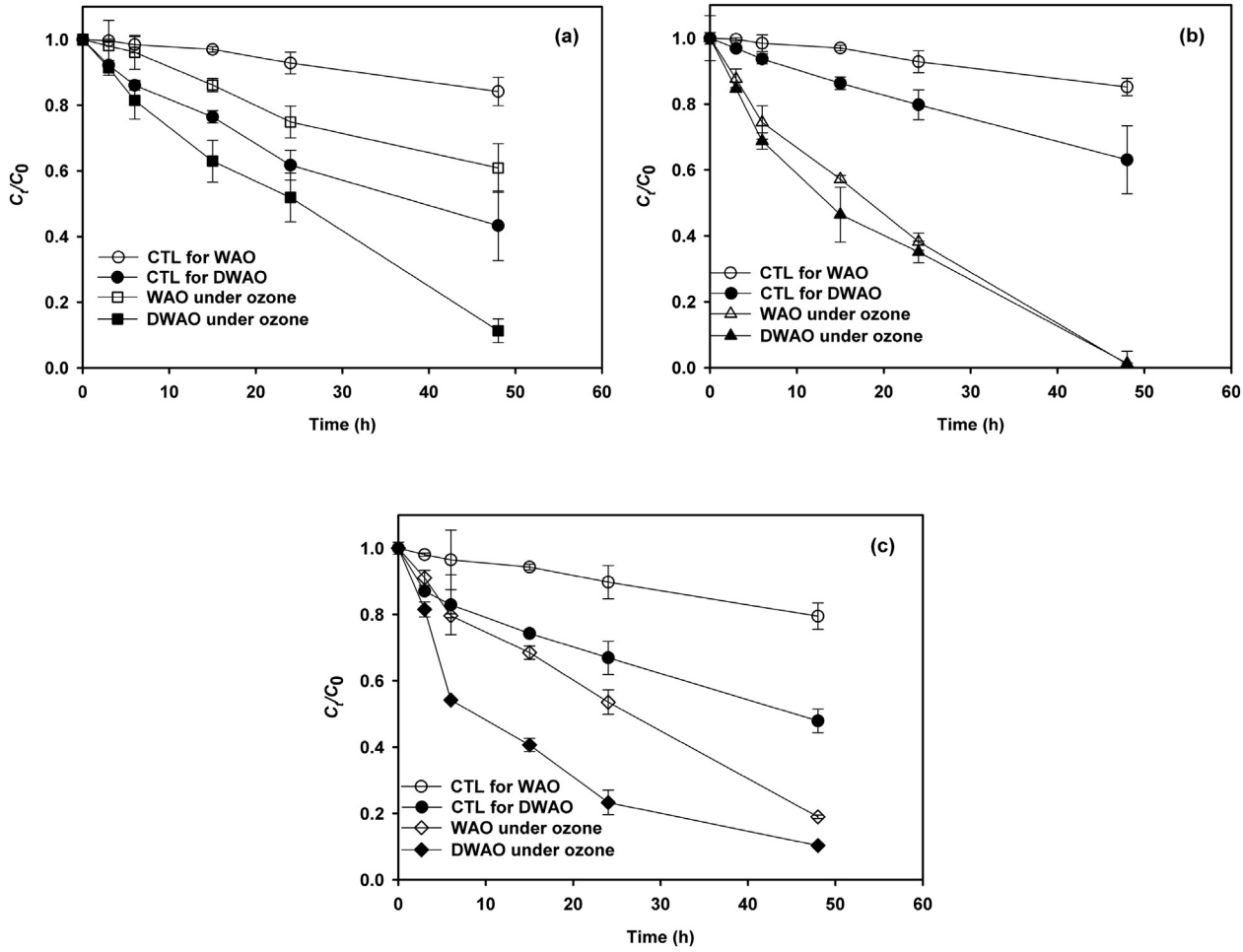

Fig. 2. Volatilization and ozonation kinetics of: (a) TPHs, (b) *n*-alkanes and (c) total PAHs in WAO and DWAO (Corexit EC9500A) solutions. Experimental conditions: For WAO, initial TPHs = 0.79 mg/L, *n*-alkanes = 0.12 mg/L and PAHs = 0.52 mg/L; For DWAO, initial TPHs = 149.70 mg/L, *n*-alkanes = 79.30 mg/L, PAHs = 6.21 mg/L, and Corexit EC9500A = 238 mg/L; ozone concentration = 86 ppbv, gas flow rate = 4 mL/min, temperature = 22 ± 1 °C, solution volume = 250 mL, pH = 8.1 ± 1, salinity = 2 wt%, and DOM = 2.2 mg/L as TOC. Symbols: experimental data plotted as mean of duplicates and error bars refer to deviation from the mean to indicate data reproducibility.

Table 1
First-order ozonation rate constants for TPHs, *n*-alkanes and total PAHs in WAO and DWAO.

Type		Volatilization		Overall dissipation		Ozonation
		k_v (h^{-1})	R^2	k (h^{-1})	R^2	k_o (h^{-1})
TPHs	WAO	0.004	0.981	0.011	0.990	0.007
	DWAO	0.018	0.992	0.034	0.975	0.016
n-Alkanes	WAO	0.003	0.986	0.045	0.974	0.041
	DWAO	0.009	0.999	0.051	0.984	0.042
Total PAHs	WAO	0.005	0.992	0.029	0.981	0.025
	DWAO	0.015	0.964	0.063	0.966	0.048

Note: R^2: coefficient of determination, $R^2 = 1\frac{\sum_i y_i - y_{i(predict)})^2}{\sum_i (y_i - \bar{y})^2}$, where y_i and $y_{i(predict)}$ are observed data and model values, respectively, and $\bar{y}$ is the mean of the observed data.

PAHs can be adequately interpreted by the pseudo first-order kinetic model ($R^2 > 0.96$). For WAO, the k_v values of TPHs, *n*-alkanes and total PAHs were determined to be 0.004, 0.003 and 0.005 h^{-1}, respectively, whereas the k_o values were 0.007, 0.041 and 0.025 h^{-1}, when exposed to 86 ppbv of ozone. For DWAO, the k_v values of TPHs, *n*-alkanes and total PAHs were elevated to 0.018, 0.009 and 0.015 h^{-1}, while the k_o values reached 0.016, 0.042 and 0.048 h^{-1}, respectively. Noting that the total oil mass in DWAO far exceeded that in WAO, the ozonation rate in DWAO was 2.2 times higher than in WAO for TPHs and PAHs, while comparable for *n*-alkanes. The elevated ozonation rates are attributed to the higher concentration, the type of dispersed hydrocarbons and the dispersant effect, as illustrated later in this section and in Section 3.3. The data revealed that the dispersed oil components are quite prone to ozonation, and thus, atmospheric ozonation can play a significant role in natural weathering of oil hydrocarbons.

Several factors can affect the ozonation rate of *n*-alkanes. First, the molecular weight or the molecular size can affect dispersibility,

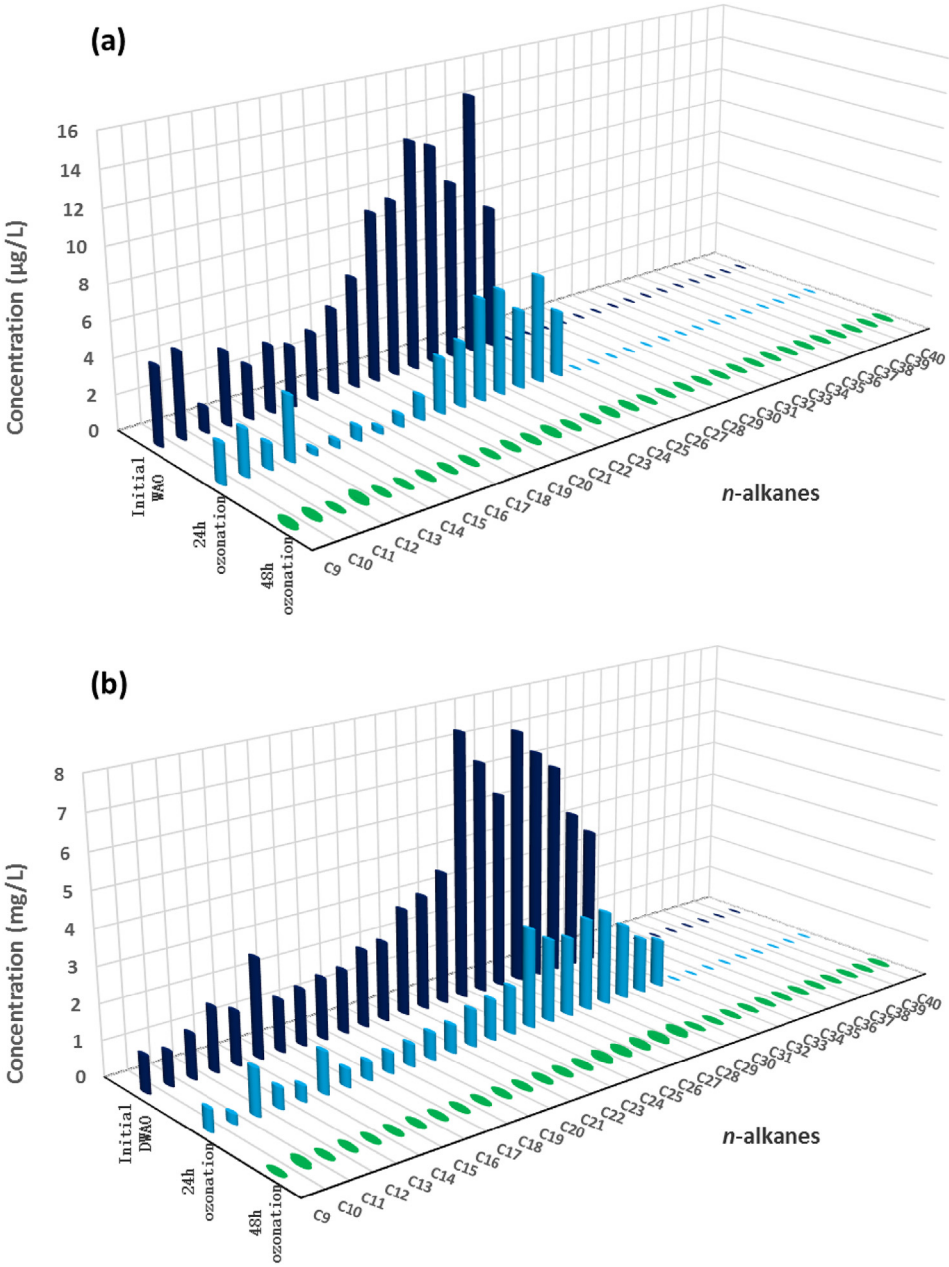

Fig. 3. Distributions of *n*-alkanes in WAO (a) and DWAO (b) before and after 48 h exposure to gaseous ozone. Experimental conditions are the same as in Fig. 2.

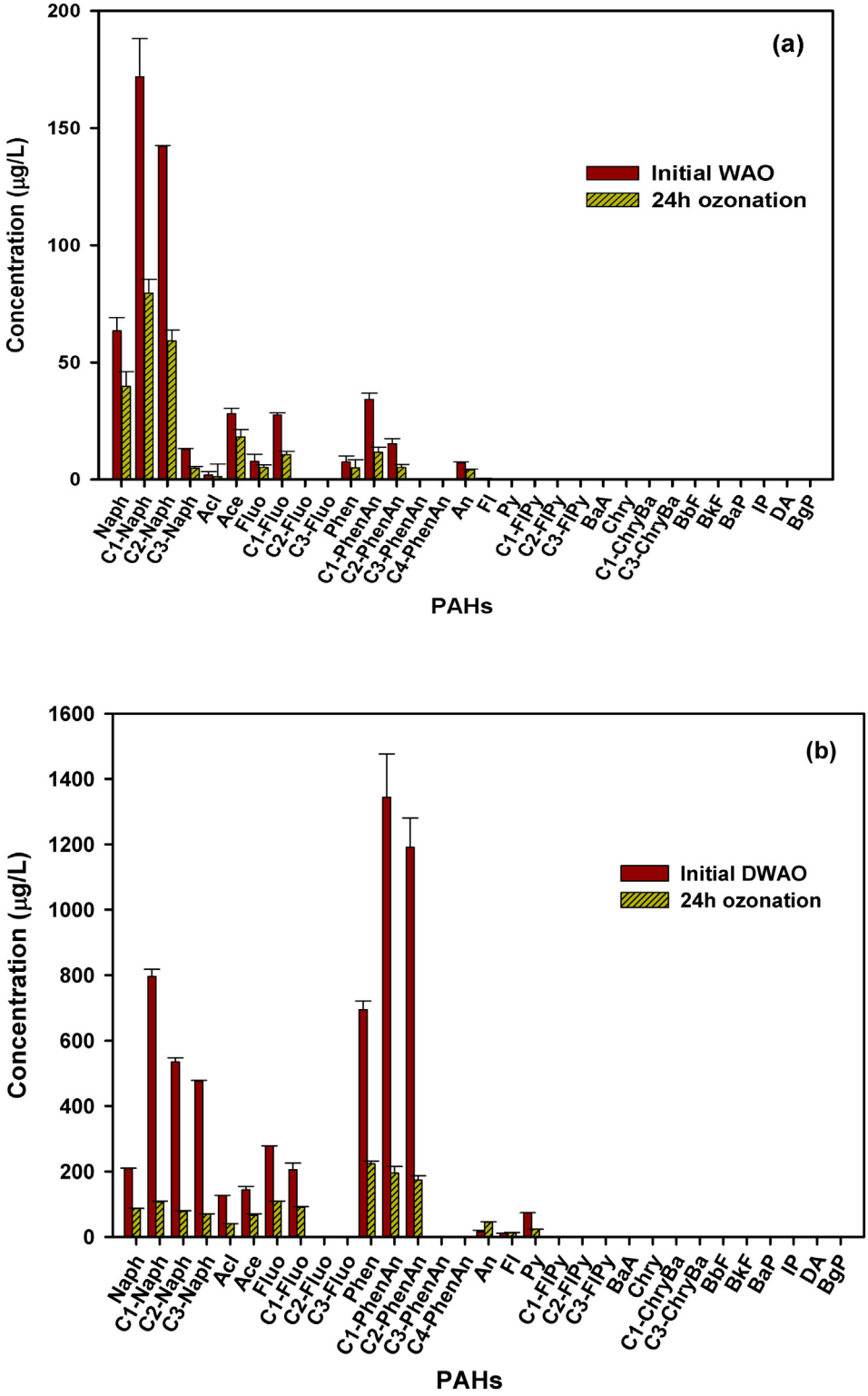

Fig. 4. Distributions of parent and alkylated PAHs in WAO (a) and DWAO (b) before and after 24 h ozonation. Experimental conditions are the same as in Fig. 2.

volatility and ozone reactivity of *n*-alkanes. In general, smaller molecules are more volatile and more vulnerable to degradation (Yin et al., 2015). In the absence of the dispersant (WAO), the oil components are truly dissolved with C19-C26 being the most abundant *n*-alkanes (Fig. 3a), and thus the volatilization rate was less than that in DWAO. While the C14-C19 fraction appeared to be more preferentially degraded in WAO, virtually all *n*-alkanes dissipated from the solution after 40 h of ozone exposure. This observation indicates that: 1) all dissolved *n*-alkanes are prone to ozonation, and 2) the high molecular weight *n*-alkanes were completely degraded without accumulation of smaller *n*-alkanes.

Second, alkyl radicals can be produced during reaction of ozonation with olefins (Hellman and Hamilton, 1974). The alkyl radicals may attack PAHs to form alkylated PAHs, also known as alkylation, resulting in decreased concentration of *n*-alkanes.

Third, the dispersant may have a profound effect on the ozonation

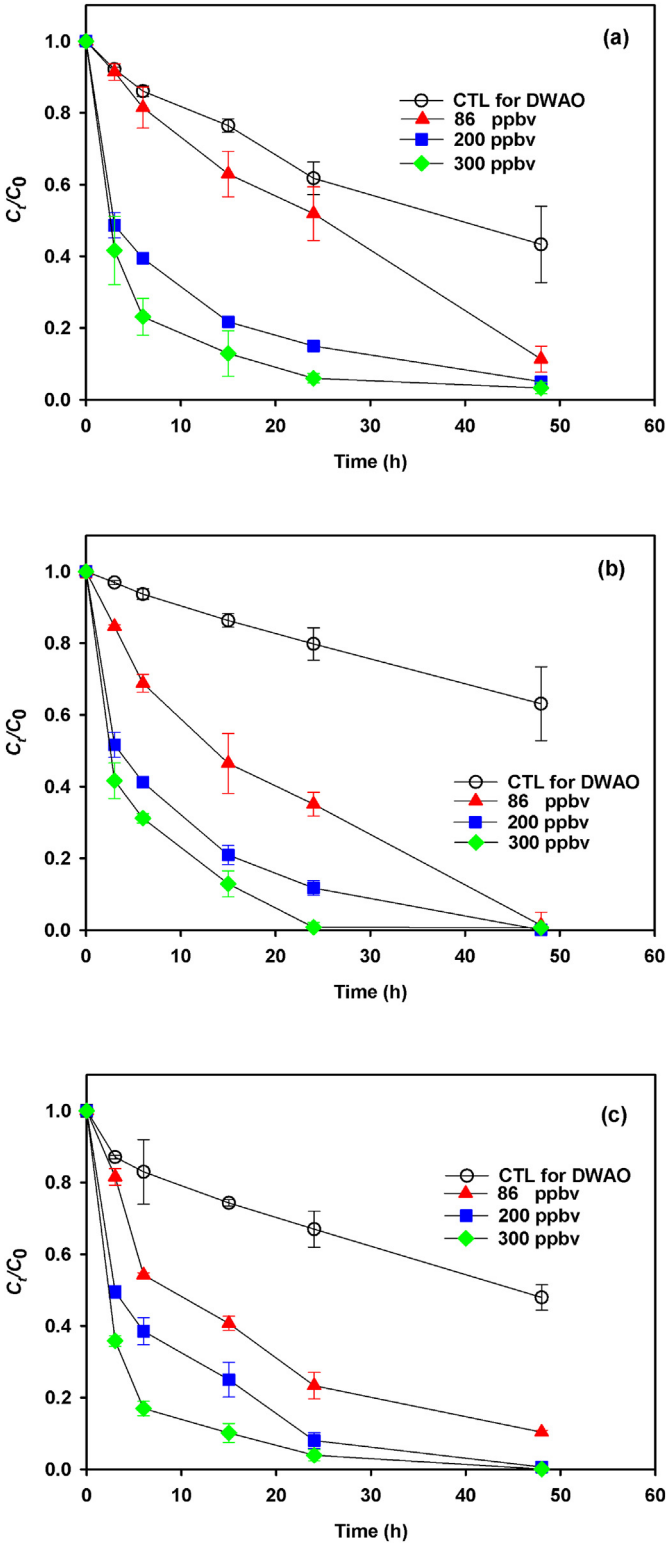

Fig. 5. Ozonation kinetics of (a) TPHs, (b) *n*-alkanes and (c) total PAHs in DWAO at various gaseous ozone concentrations. Experimental conditions: Initial TPHs = 149.70 mg/L, *n*-alkanes = 79.30 mg/L, PAHs = 6.21 mg/L, Corexit EC9500A = 238 mg/L, gas flow rate = 4 mL/min, temperature = 22 ± 1 °C, solution volume = 250 mL, pH = 8.1 ± 1, salinity = 2 wt%, and DOM = 2.2 mg/L TOC. Symbols: experimental data plotted as mean of duplicates and error bars refer to deviation from the mean to indicate data reproducibility.

process. In the presence of the dispersant, much more oil is dispersed, and the component distribution in DWAO appeared quite similar to that of WAO as well as in the crude oil (Zhao et al., 2016). However, dispersed *n*-alkanes were more volatile than the dissolved *n*-alkanes (Fig. 2). As the dispersion of *n*-alkanes involves π-π interactions and/or hydrophobic interactions between *n*-alkanes and the dispersant aggregates and/or micelles, the medium-molecular-weight (e.g., C24-C30) fraction of *n*-alkanes is preferably dispersed (in this study, the C24-C30 fraction accounted for 61.1% of the total *n*-alkanes) (Fig. 3b). The higher concentration and higher volatility of the dispersed *n*-alkanes are more conducive to both direct and indirect ozonation, where larger *n*-alkanes are transformed to the smaller homologs and then mineralized (Vikhorev et al., 1978). On the other hand, the mass transfer rate of larger *n*-alkanes is slower than that of smaller *n*-alkanes, which can be further slowed down due to the attachment of the dispersant molecules, resulting in slower degradation for larger *n*-alkanes. Moreover, the dispersant can increase soluble ozone concentration and enhance the radical generation, especially superoxide radicals (Gong and Zhao, 2017); on the other hand, the dispersant may also compete for the reactive species. As the dispersant lowers the surface tension of water, it reduces the ozone mass transfer resistance at the ozone-water interface, which may increase both direct ozonation and generation of radicals in the aqueous phase (Chu et al., 2006; Gong and Zhao, 2017). Lastly, the dispersant (mainly Span 80) can facilitate accumulation of more hydrophobic hydrocarbons to the upper layer of the water column in the reactor, promoting the exposure to the gaseous ozone, and thus the ozonation reactions (Fu et al., 2017).

Compared to *n*-alkanes, the dispersant was much less effective in dispersing PAHs. Fig. 4 displays the distributions of PAHs in WAO and DWAO before and after ozonation. The initial concentrations of parent PAHs and alkylated PAHs were 0.12 and 0.41 mg/L in WAO, which were raised to 1.34 and 4.82 mg/L in DWAO, respectively. Notably, the 2-ring and 3-ring PAHs and their alkylated PAHs (e.g., C1-naphthalene, C2-naphthalene, C3-naphthalene, C1-phenanthrene and C2-phenanthrene) were preferably dispersed in DWAO. Phenanthrene (Phen) is the most abundant parent PAH, accounting for 11.3% of the total PAHs, followed by fluorene (Fluo) (4.5%), naphthalene (3.4%) and acenaphthene (Ace) (2.3%). The 3-ring PAHs make up 22.3% of the total PAHs. The concentration of total alkylated PAHs was 3.6 times higher than total parent PAHs, which is consistent with other studies (Yin et al., 2015; Zhao et al., 2016).

The ozonation rates for both parent and alkylated PAHs in DWAO were much faster than in WAO, especially for the 2-ring (naphthalene), 3-ring (acenaphthylene, fluorene and phenanthrene) and 4-ring (fluoranthene and pyrene) PAHs and their alkylated homologs (Fig. 4, Fig. S2 and Table S3 in SM).

For instance, the 24-h degradation of Naph, C1-Naph, C2-Naph, and C3-Naph reached 37.3%, 53.7%, 58.4%, and 62.1%, respectively in WAO, which was elevated to 58.3%, 86.7%, 85.4%, and 85.4% in DWAO. Moreover, the alkylated PAHs were more effectively degraded than their parent homologs in both WAO and DWAO; and the most degradation was observed for alkylated naphthalenes (85.4%–86.7%), alkylated phenanthrenes/anthracenes (84.5%), and alkylated fluoranthrenes/pyrenes (100%) in DWAO.

Bacosa et al. (2015) studied photodegradation of dispersed oil hydrocarbons, and they observed some similar degradation patterns. For instance, they found that 3-ring PAHs were more sensitive to photooxidation than 4- to 5-ring PAHs, and that except for phenanthrene, 3-ring PAHs were degraded faster than naphthalene. Moreover, they observed that alkylated pyrenes were photodegraded faster than alkylated phenanthrenes, while alkylated naphthalenes were degraded faster than alkylated phenanthrenes; and alkylated PAHs were photodegraded faster than their parent homologs. These similarities suggest that ozonation and photodegradation of dispersed oil hydrocarbons may share some common reaction mechanisms such as degradation facilitated by radicals.

Moreover, the volatilization rates of parent and alkylated PAHs in DWAO were 4 and 2 times higher than in WAO. This can be attributed to the much higher concentration of the 2-ring PAHs in DWAO, which are known to be more volatile (Liu et al., 2012). At 48 h, the volatilization loss of parent PAHs in WAO and DWAO was 24.9% and 66.9%, respectively, compared to 6.3% and 36.3% for alkylated PAHs, indicating that like *n*-alkanes, dispersed PAHs are more volatile than the dissolved counterparts. The overall depletion was 77.0% and 86.7% for the parent PAHs in WAO and DWAO, respectively, and 97.4% and 92.5% for alkylated PAHs, indicating that alkylated PAHs are more vulnerable to ozonation than the parent PAHs and that dispersed PAHs are more prone to ozonation than the dissolved counterparts. Mechanistically, the dissolution/dispersion and ozonation of PAHs can be affected by the following factors: First, the lower abundance of PAHs in oil hydrocarbons may result in the lower dispersion of PAHs than *n*-alkanes by the dispersant (Zhao et al., 2016). Second, the hydrophile-lipophile balance (HLB) values of the different surfactants in Corexit EC9500A range from 4.3 to 15 (Table S2); as such, the dispersant is more favorable towards *n*-alkanes than PAHs (Couillard et al., 2005; Diallo et al., 1994). Third, more hydrophobic PAHs (i.e. larger PAHs) tend to resist the dispersing and ozonation processes (Walter et al., 2000). Fourth, the presence of ozone may cause alkylation of the parent PAHs, resulting in a rise in alkylated PAHs (Lima et al., 2005; Ringuet et al., 2012; Zhao et al., 2016). This assertion is supported by Fig. S3 in SM, which shows a faster removal rate of parent PAHs than alkylated PAHs in the early stage (< 15 h). After 15 h, or upon completion of the initial alkylation of the parent PAHs, the ozonation rate increased sharply, indicating alkylated PAHs are more ozone-reactive than the corresponding parent PAHs.

The dispersant effects on the ozonation of PAHs followed a similar manner as for *n*-alkanes, although the extents differed due to their different molecular characteristics.

3.2. Degradation of oil hydrocarbons in DWAO at various atmospheric ozone concentrations

Fig. 5 shows ozonation kinetics of TPHs (Fig. 5a), *n*-alkanes (Fig. 5b) and PAHs (Fig. 5c) in DWAO when exposed to various gaseous ozone concentrations but at a fixed gas flowrate 4 mL/min. The overall removal rate of the oil components increased with increasing ozone concentration. As the ozone concentration increased from 86 to 300 ppbv, the rate constant k_o was boosted from 0.016 to 0.237 h^{-1} for TPHs (by 14.8 times), from 0.042 to 0.210 h^{-1} for *n*-alkanes (by 5.1 times) and from 0.048 to 0.302 h^{-1} for total PAHs (by 6.3 times) (Table 2). According to the Henry's law, the higher gaseous ozone concentration results in higher soluble ozone in the aqueous phase, leading to more accessible molecule ozone and free radicals. However, the effect of ozone concentration became less profound at O_3 > 200 ppbv, suggesting that mass transfer became more important at elevated O_3 concentration. In addition, the ozone-facilitated alkylation rate may also be enhanced at higher ozone concentrations.

Table 2
First-order ozonation rate constants for TPHs, *n*-alkanes and TPAHs in DWAO at various concentrations of simulated atmospheric ozone.

Type	Ozone (ppbv)	Volatilization		Overall dissipation		Ozonation
		k_v (h^{-1})	R^2	k (h^{-1})	R^2	k_o (h^{-1})
TPHs	86	0.018	0.992	0.034	0.975	0.016
	200	0.018	0.992	0.136	0.919	0.118
	300	0.018	0.992	0.254	0.973	0.237
n-alkanes	86	0.009	0.999	0.051	0.984	0.042
	200	0.009	0.999	0.134	0.954	0.124
	300	0.009	0.999	0.220	0.972	0.210
Total PAHs	86	0.015	0.964	0.063	0.966	0.048
	200	0.015	0.964	0.138	0.939	0.124
	300	0.015	0.964	0.316	0.984	0.302

3.3. Effect of dispersant concentration on ozonation of petroleum hydrocarbons in DWAO

Fig. 6 shows the remaining concentrations of TPHs, *n*-alkanes and PAHs in DWAO after 24 h of ozonation when additional 18 or 24 mg/L of Corexit EC9500A was added to the DWAO. Fig. 6a shows that the addition of the dispersant resulted in much lower concentrations of TPHs and *n*-alkanes, and the addition of 18 and 24 mg/L of the dispersant gave comparable results. The findings indicate that the addition of excess dispersant enhances ozonation of TPHs and *n*-alkanes. However, there exists a threshold concentration, above which the dispersant effect becomes less significant. Fig. 6c shows that the dispersant promotes ozonation of > C20 *n*-alkanes to a greater extend. The favorable effects of the dispersant on TPHs and *n*-alkanes are attributed to the mechanisms discussed in Section 3.1. However, the degradation for PAHs was inhibited at the elevated dispersant concentrations (Fig. 6a and b). After 24 h of ozonation, the final concentrations of parent PAHs were 0.61, 0.72 and 0.71 mg/L when 0, 18, and 24 mg/L of the dispersant were added, respectively; and the final concentrations of alkylated PAHs were 0.71, 1.91 and 1.94 mg/L. Increasing the dispersant concentration from 0 to 18 mg/L decreased the degradation of total PAHs from 78.6% to 57.0%, parent PAHs from 54.8% to 47.4%, and alkylated PAHs from 85.2% to 59.6%. Further increasing the dispersant addition to 24 mg/L had insignificant further effect. Fig. 6d shows that such inhibitive effects at elevated dispersant concentrations occurred mainly to the 2-ring and 3-ring alkylated PAHs.

The critical micelle concentration (CMC) of Corexit EC9500A was reported to be 22.5 mg/L (Gong et al., 2014). Our results suggest that both *n*-alkanes and PAHs can interact with the dispersant molecules strongly even below the CMC. PAHs are intrinsically more stable due to the π electrons delocalized over the aromatic rings than *n*-alkanes (Rubio-Clemente et al., 2014). The 3-rings PAHs are the dominant components for both parent and alkylated PAHs. These relatively smaller aromatic compounds may undergo the “caging effect”, i.e., partitioning into the surfactant (e.g., Span 80) aggregates/micelles, which retards the encountering between ozone molecules/radicals and PAHs. (Fu et al., 2017; Zhang et al., 2011). The effect is less significant for *n*-alkanes due to their chain-like structures. In addition, the rise in alkylated PAHs at elevated dispersant concentrations can also be due to the fact that while elevated dispersant concertation facilitates alkylation of parent PAHs due to generation of more alkyl radicals, the high dispersant concentration can also inhibit the subsequent degradation of the alkylated PAHs due to the caging effect.

To determine the effect of the dispersant on production of ·OH radicals, *p*CBA was used as a probe chemical and an ·OH scavenger to measure the ·OH radicals (details are described in Section 3.5). Fig. 7 shows ozone-oxidation of *p*CBA during ozonation with or without the dispersant. It is evident that the presence of 18 mg/L of the dispersant significantly enhanced the degradation of *p*CBA ($P = 0.003$ at the 0.05 level of significance), indicating enhanced generation of hydroxyl radicals. However, further increasing the dispersant to 24 mg/L (higher than the CMC value) resulted in less ozonation of *p*CBA, or a statistically insignificant change in the reaction rate ($P = 0.852$) compared to that without dispersant. This inhibitive effect at 24 mg/L of the dispersant may be attributed to: 1) the formation of micelles may exert the caging effect, which retards the decomposition of soluble ozone (Eriksson, 2005), and 2) elevated competition of the dispersant for the free radicals at higher dispersant concentrations.

3.4. Effects of water chemistry on ozonation of petroleum hydrocarbons in DWAO

3.4.1. Effects of pH

Fig. 8 shows the concentrations of TPHs, *n*-alkanes and total PAHs in DWAO at various pH levels (6.0, 7.0, 8.0, and 9.0) after 24 h of exposure to 86 ppbv of gaseous ozone. The overall dissipation rate of

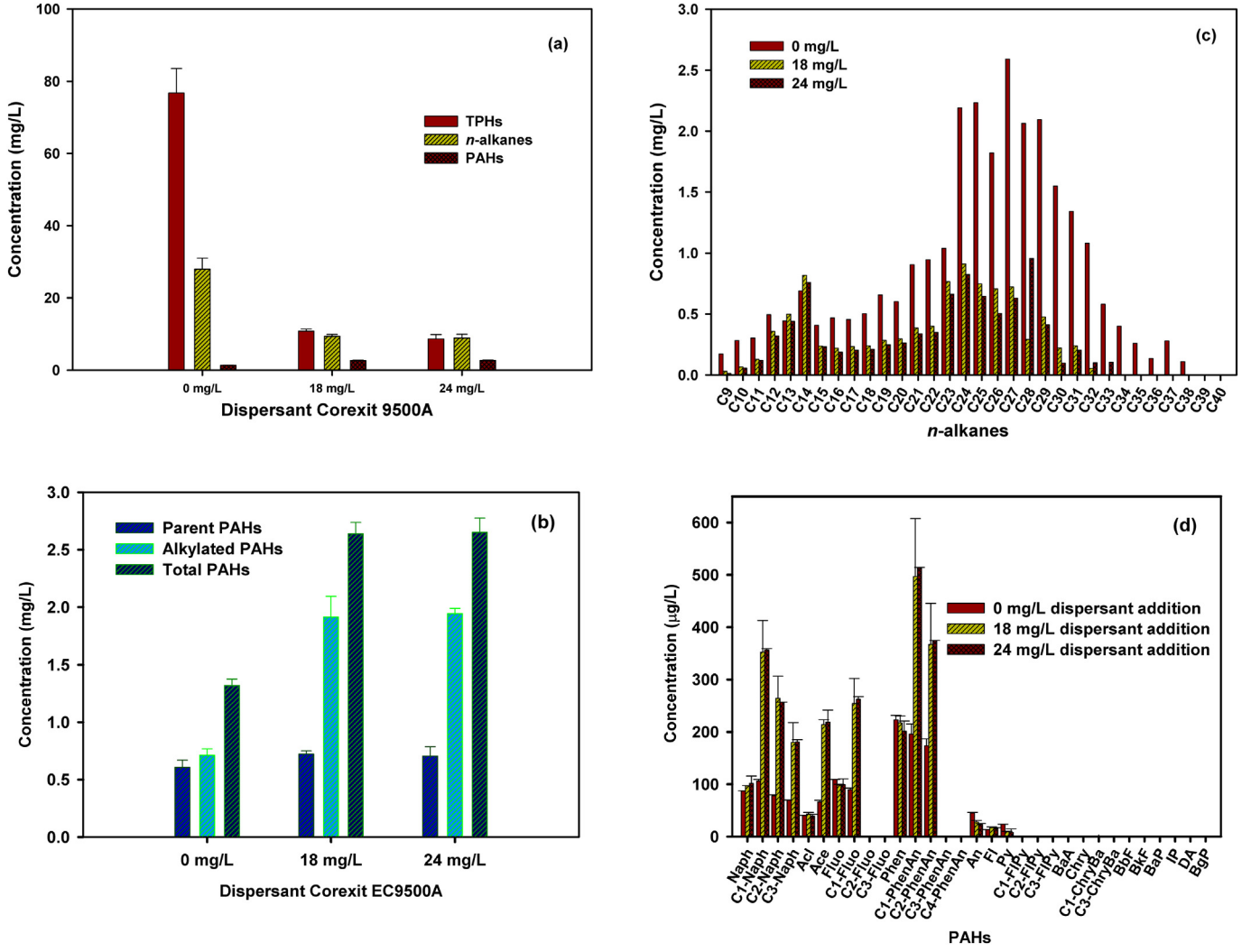

Fig. 6. Remaining concentrations of TPHs, *n*-alkanes and total PAHs (a), and parent PAHs and alkylated PAHs (b) in DWAO after 24 h ozonation in the presence of various concentrations of the dispersant, and distributions of *n*-alkanes (c) and PAHs (d) in DWAO after 24 h ozonation. Experimental conditions: Initial TPHs = 149.70 mg/L, *n*-alkanes = 79.30 mg/L and total PAHs = 6.21 mg/L, Corexit EC9500A = 238 mg/L, gas flow rate = 4 mL/min, gaseous ozone = 86 ppbv, temperature = 22 ± 1 °C, solution volume = 250 mL, solution pH = 8.1 ± 1, salinity = 2 wt%, and DOM = 2.2 mg/L as TOC. Symbols: experimental data plotted as mean of duplicates and error bars refer to deviation from the mean to indicate data reproducibility.

TPHs, *n*-alkanes and PAHs decreased from 59.7% to 46.2% ($P = 0.003$ at the 0.05 level of significance), from 66.3% to 61.5% ($P = 0.078$) (Fig. S5) and from 87.8% to 86.9% ($P = 0.551$) (Figs. S4 and S5), respectively, when the solution pH was increased from 6.0 to 9.0, indicating an inhibitive effect at higher pH in the tested pH range. It has been well known that solution pH can affect both direct and indirect ozonation reactions (Zhao et al., 2011). As pH increases, the aqueous ozone decomposes via the reactions as shown in Eqs. (2)–(6) (Kasprzyk-Hordern et al., 2003):

$$O_3 + H_2O \rightarrow 2{\cdot}OH + O_2 \quad (2)$$

$$O_3 + OH^- \rightarrow HO_2{\cdot} + {\cdot}O_2^- \quad (3)$$

$$O_3 + {\cdot}OH \rightarrow HO_2{\cdot} + O_2 \leftrightarrow 2{\cdot}O_2^- + H^+ \quad (4)$$

$$O_3 + HO_2{\cdot} \rightarrow 2O_2 + {\cdot}OH \quad (5)$$

$$2HO_2{\cdot} \rightarrow O_2 + H_2O_2 \quad (6)$$

Alkaline conditions favor aqueous ozone decomposition to form more free radicals including hydroxyl radicals and superoxide radicals (Eqs. (3)–(4)), and thus enhances the indirect ozonation. However, direct ozonation is compromised due to consumption of molecular ozone. Because direct ozonation is the predominant process for oxidation of TPHs (Direct ozonation accounted for 53% of the overall ozonation), the lessened direct ozonation resulted in the observed inhibitive effect at higher pH. However, depending on the different ozonation mechanisms, such pH effects can vary. For instance, Beltran et al. (1995) reported that the ozone oxidation rate of fluorene increased with increasing pH; however, Gong and Zhao (2017) observed that ozonation of pyrene in the presence of the same dispersant decreased with increasing pH. They claimed that this discordance may result from the dispersant effect, which can compete for the radicals more intensely than for the ozone molecules, thus inhibiting indirect ozonation.

3.4.2. Effects of humic acid

Fig. 9 shows ozonation kinetics of TPHs in DWAO with 0.5, 1.0 or 5.0 mg/L as TOC of humic acid added and at a gaseous ozone concentration of 200 ppbv. After 24 h of exposure to the nitrogen gas flow, the volatilization loss of TPHs in DWAO was 38.2% in all cases, whereas the overall depletion of TPHs was 93.4%, 89.9% and 74.6%, respectively, in the presence of 0.5, 1.0 and 5.0 mg/L humic acid and when exposed to the gaseous ozone. Table 3 presents the respective rate constants for overall depletion, volatilization and ozonation. When 5.0 mg/L of humic acid was added, the overall dissipation rate constant

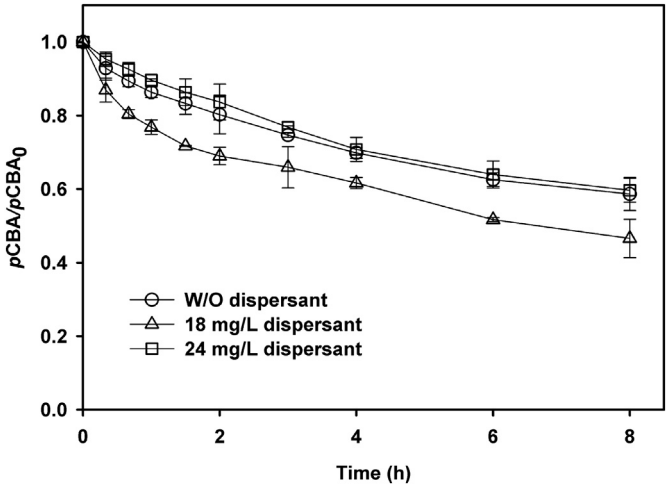

Fig. 7. Oxidation of *p*CBA (normalized to initial concentration) during ozonation with or without 18 or 24 mg/L of Corexit EC9500A in seawater. Experimental conditions: Gas flow rate = 4 mL/min, gaseous ozone = 86 ppbv, initial *p*CBA concentration = 3 μM, temperature = 22 ± 1 °C, solution volume = 250 mL, salinity = 2 wt%, and DOM = 2.2 mg/L as TOC. Symbols: experimental data plotted as mean of duplicates and error bars refer to deviation from the mean to indicate data reproducibility.

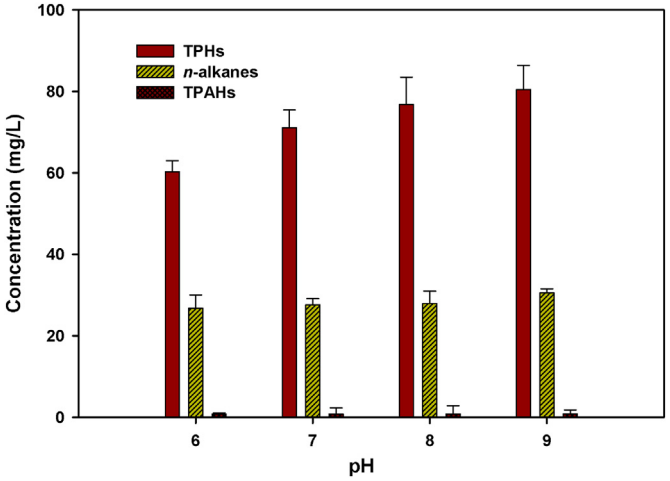

Fig. 8. Remaining concentrations of TPHs, *n*-alkanes and total PAHs in DWAO after 24 h ozonation at various initial pH levels. Experimental conditions: Initial TPHs = 149.70 mg/L, *n*-alkanes = 79.30 mg/L and total PAHs = 6.21 mg/L, Corexit EC9500A = 238 mg/L, gas flow rate = 4 mL/min, gaseous ozone = 86 ppbv, temperature = 22 ± 1 °C, solution volume = 250 mL, salinity = 2 wt%, and DOM = 2.2 mg/L as TOC. Symbols: experimental data plotted as mean of duplicates and error bars refer to deviation from the mean to indicate data reproducibility.

(k) was decreased from 0.136 to 0.051 h^{-1}, and the ozonation rate constant (k_o) from 0.118 h^{-1} to 0.032 h^{-1} (Table 3). The distribution of different segments of *n*-alkanes after 24 h of ozonation (Fig. S6a) indicates that the inhibitive effect of humic acid was more evident on the larger *n*-alkanes, in particular the C24-C30 fraction; and the higher TOC concentration, the less these lager *n*-alkanes were degraded. Fig. S6b shows the distributions of PAHs after 24 h of ozonation at various humic acid concentrations. The remaining concentrations of parent PAHs were 3.0, 8.9, 17.0 and 18.4 mg/L, respectively, when 0.5, 1.0, 5.0, and 10 mg/L as TOC of humic acid were added. Evidently, more 3-ring PAHs (acenaphthene, fluorene and phenanthrene) remained after the ozonation at higher humic acid concentrations (5.0 or 10 mg/L), indicating degradation of these PAHs were inhibited to a greater extent. The inhibitive effect on 2-ring PAHs (naphthalene) was much less, and

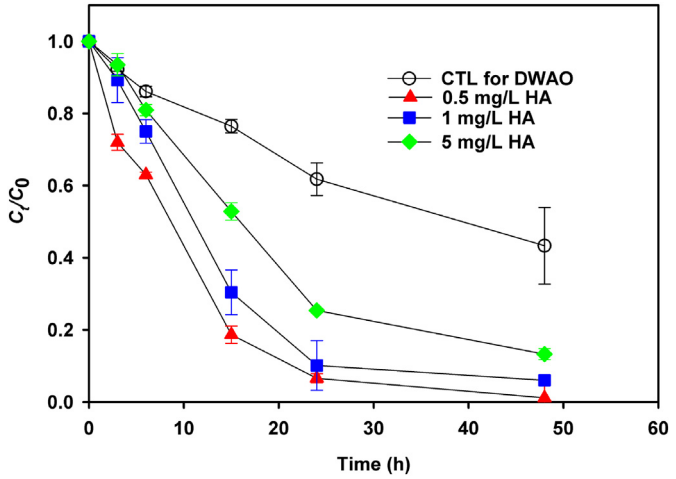

Fig. 9. Effect of HA on ozonation of TPHs in DWAO. Experimental conditions: Initial TPHs = 149.7 mg/L, *n*-alkanes = 79.3 mg/L and total PAHs = 6.21 mg/L (in DWAO with Corexit EC9500A), gas flow rate = 4 mL/min, ozone concentration = 200 ppbv, temperature = 22 ± 1 °C, volume of solution = 250 mL, solution pH = 8.1 ± 1, salinity = 2.0 wt%, and DOM = 2.2 mg/L as TOC. Symbols: experimental data plotted as mean of duplicates and error bars refer to deviation from the mean to indicate data reproducibility.

Table 3
First-order ozonation rate constants for TPHs in DWAO in the presence of various concentrations of humic acid.

HA concentration	Volatilization		Overall dissipation		Ozonation
	k_v (h^{-1})	R^2	k (h^{-1})	R^2	k_o (h^{-1})
0 mg/L	0.018	0.992	0.136	0.919	0.118
0.5 mg/L	0.018	0.992	0.100	0.985	0.082
1 mg/L	0.018	0.992	0.077	0.970	0.059
5 mg/L	0.018	0.992	0.050	0.976	0.032

there was virtually no effect on the 2-ring alkyl homologs (C1-naphthalene, C2-naphthalene and C3-naphthalene).

DOM can affect soluble ozone stability in three ways: 1) directly react with soluble ozone (Eqs. (7) and (8)) (von Gunten, 2003) and therefore compete for molecular ozone with the target hydrocarbons; 2) acting as a promoter to convert the nonselective hydroxyl radicals into superoxide radicals (Eqs. (9) and (10)) (Staehelin and Hoigne, 1985; von Gunten, 2003), resulting in a net loss in the indirect ozonation becuase the oxidation power of superoxide radicals is lower than that of hydroxyl radicals (Litter and Quici, 2010); and 3) sorption of some oil components (e.g., PAHs) within the complex HA matrix may shield it from the molecular ozone and free radicals (Simpson et al., 2004).

$$O_3 + NOM1 \rightarrow NOM1_{ox} \quad (7)$$

$$O_3 + NOM2 \rightarrow NOM2^{\cdot+} + \cdot O_3^- \quad (8)$$

$$\cdot OH + NOM3 \rightarrow NOM3\cdot + H_2O \text{ or } NOM4\cdot + OH^- \quad (9)$$

$$NOM3 + O_2 \rightarrow NOM - \cdot O_2 \rightarrow NOM3^+ + \cdot O_2^- \quad (10)$$

3.4.3. Effects of salinity

Fig. 10 shows the effects of salinity on ozonation of TPHs, *n*-alkanes and total PAHs in DWAO. The overall dissipation of all the oil components after 24 h of ozonation was increased when the solution salinity was increased from 2.0% to 8.0%, namely, from 48.1% to 53.7% for TPHs (P = 0.058), from 64.8 to 74.2% for *n*-alkanes (P = 0.022), and from 78.8% to 84% for total PAHs (P = 0.065). Fig. S7 shows the distributions of *n*-alkanes and PAHs in DWAO after 24-h ozonation and at

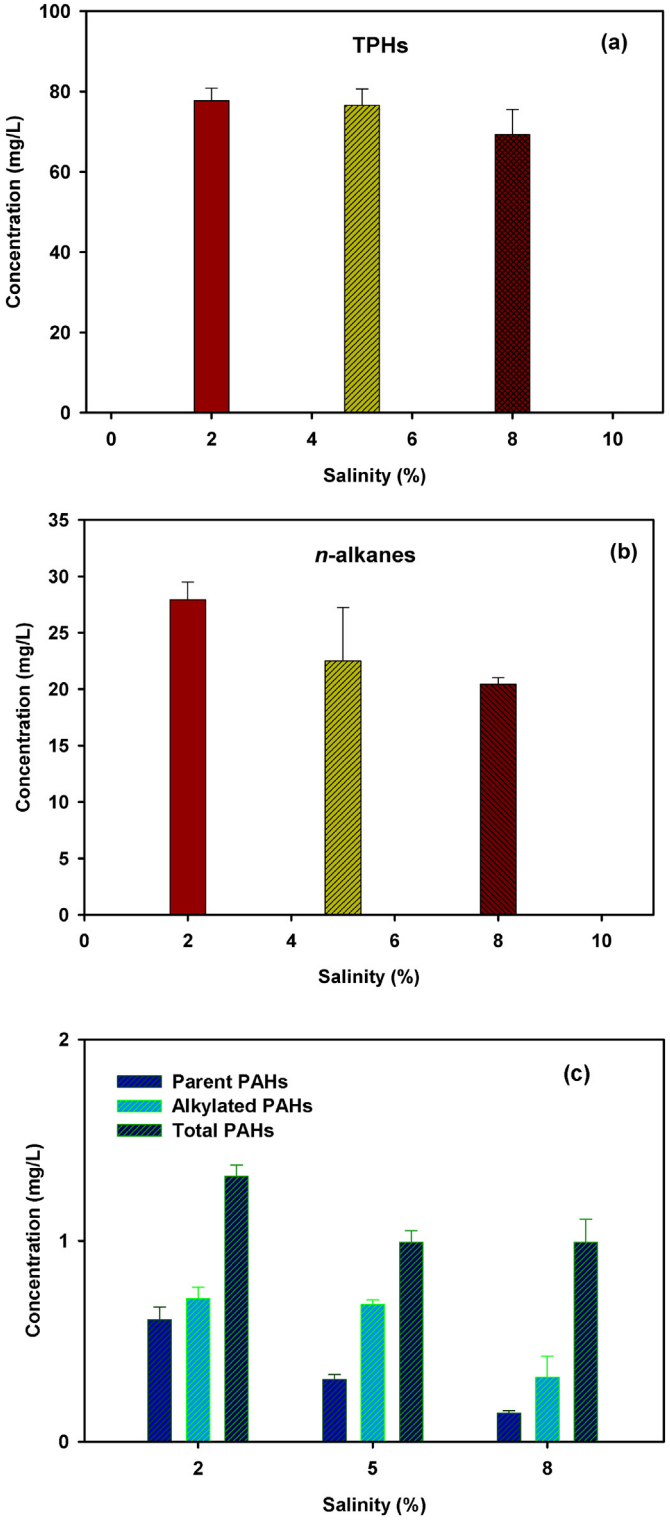

Fig. 10. Remaining concentrations of: (a) TPHs, (b) *n*-alkanes and (c) PAHs in DWAO after 24-h ozonation at various salinity levels. Experimental conditions: Initial TPHs = 149.7 mg/L, *n*-alkanes = 79.3 mg/L and total PAHs = 6.2 mg/L (in DWAO with Corexit EC9500A), gas flow rate = 4 mL/min, ozone concentration = 86 ppbv, temperature = 22 ± 1 °C, volume of solution = 250 mL, solution pH = 8.1 ± 1, and DOM = 2.2 mg/L as TOC. Symbols: experimental data plotted as mean of duplicates and error bars refer to deviation from the mean to indicate data reproducibility.

various salinity levels. Evidently, the most salinity effects occurred to the < C14 or > C24 *n*-alkanes.

Salinity can affect ozone oxidation of oil components in the dispersant solutions in some contrasting ways (Gong and Zhao, 2017). First, NaCl can compete for dissolved ozone and radicals. As such, high salinity results in more inhibition of the ozonation on oil hydrocarbons (Muthukumar and Selvakumar, 2004). Second, elevated IS can increase the interfacial concentration of oil hydrocarbons at the ozone-solution interface due to the "salting out effect", which enhances degradation of oil hydrocarbons. However, in the presence of the dispersant, the "salting out" effect is partially offset due to lowered surface tension and enhanced solubilization of the hydrophobic oil compounds. Third, in the presence of the dispersant, some of the lighter and less-soluble components in the dispersant (e.g., Span 80) may entrain more oil hydrocarbons to the top layer of the water column, which is conducive to the contact and reactions with gaseous ozone in the headspace. Fourth, elevated IS may push more oil compounds to the dispersant/solvent cages, inhibiting ozonation.

3.5. Ozonation mechanisms

Typically, the radicals are formed through the following reactions (Forni et al., 1982; von Gunten, 2003; Zhao et al., 2004).

$$O_3 + OH^- \rightarrow HO_2^- + O_2 \quad (11)$$

$$O_3 + HO_2^- \rightarrow \cdot OH + \cdot O_2^- + O_2 \quad (12)$$

$$O_3 + \cdot O_2^- \rightarrow \cdot O_3^- + O_2 \quad (13)$$

$$\cdot OH + O_3 \rightarrow HO_2\cdot + O_2 \quad (14)$$

$$\cdot O_3^- + H_2O \leftrightarrow O_2 + \cdot OH + OH^- \quad (15)$$

It is worth noting that the oxidation power of superoxide, ozonide and hydroperoxyl radicals is lower than that of hydroxyl radicals ($E^0 = +2.86$ V) (Litter and Quici, 2010).

To quantify the relative contributions of direct and indirect ozonation mechanisms, ozonation kinetics of TPHs, *n*-alkanes and total PAHs were measured with *p*CBA as an ·OH scavenger and with or without the dispersant. Eqs. (16) and (17) illustrates reactions of *p*CBA with ·OH, and the second-order rate constant has been reported to be $k_{\cdot OH,pCBA} = 5.2 \times 10^9\ M^{-1}\ s^{-1}$ (Elovitz et al., 2000). The steady-state concentration of ·OH ($[\cdot OH]_{ss}$) is calculated based on the depletion rate of *p*CBA according to Eq. (18) (von Gunten, 2003; Zhang et al., 2013):

$$p\text{CBA} + \cdot OH \rightarrow Intermediates \quad (16)$$

$$-\frac{d[p\text{CBA}]}{dt} = k_{\cdot OH,p\text{CBA}}[p\text{CBA}][\cdot OH]_{ss} \quad (17)$$

$$k_{\cdot OH,p\text{CBA}}[\cdot OH]_{ss} = k_{obs,p\text{CBA}} \quad (18)$$

where the $k_{obs,pCBA}$ is the pseudo-first-order rate constant of *p*CBA degradation, which is 0.029 h^{-1} (Eq. (1) was employed to fit the experimental data in Fig. 11).

The overall TPHs depletion, involving volatilization, direct ozone oxidation and indirect radical oxidation, can be described by:

$$\frac{dC}{dt} = (k_v + k_D + k_R)C \quad (19)$$

where C is the reactant concentration (μg/L) at time t (h); and k_v, k_D and k_R refer to the rate constants (h^{-1}) of volatilization, direct ozonation and indirect ozonation.

Fig. 11 compares the overall ozonation and direct ozonation rates of TPHs (Fig. 11a), *n*-alkanes (Fig. 11b), and total PAHs (Fig. 11c), and Table 4 gives the respective rate constants due to volatilization and different ozonation mechanisms. In the absence of *p*CBA, the overall ozonation rate constant of TPHs was 0.016 h^{-1}; in the presence of the

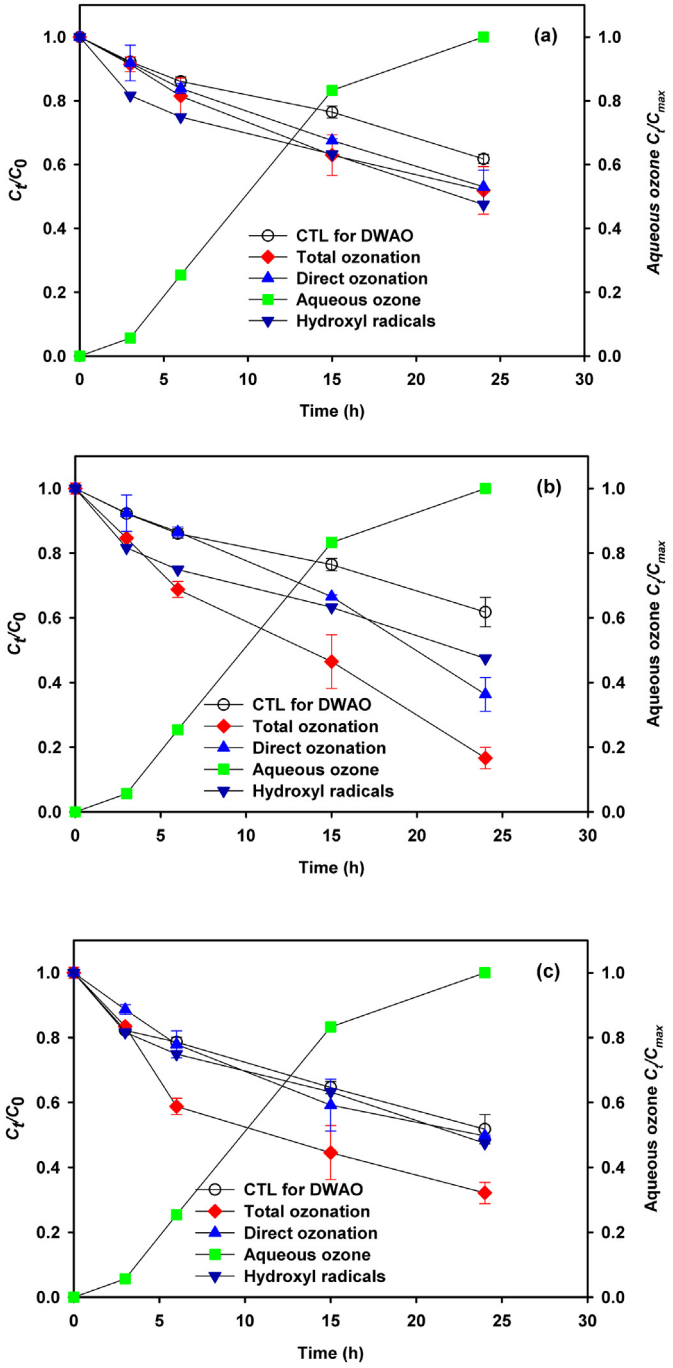

Fig. 11. Transformation of (a) TPHs, (b) *n*-alkanes and (c) total PAHs by molecular ozone and hydroxyl radicals during ozonation of DWAO. Experimental conditions: Initial TPHs = 149.7 mg/L, *n*-alkanes = 79.3 mg/L and total PAHs = 6.2 mg/L (in DWAO with Corexit EC9500A), gas flow rate = 4 mL/min, ozone concentration = 86 ppbv, temperature = 22 ± 1 °C, volume of solution = 250 mL, solution pH = 8.1 ± 1, salinity = 2.0 wt% and DOM = 2.2 mg/L as TOC.

*p*CBA, the ozonation (direct ozonation) rate constant of TPHs was reduced to 0.009 h^{-1}, indicating that direct ozonation accounted for 56% of the overall ozonation based on the pseudo first-order rate constant. Fig. 11b shows the volatilization, total ozonation and direct ozonation of *n*-alkanes in DWAO. In the absence of the *p*CBA, the total ozonation rate of *n*-alkanes was 0.033 h^{-1}; in the presence of *p*CBA, the ozonation rate was reduced to 0.018 h^{-1}, namely, 55% of the overall ozonation was attributed to direct ozonation, indicating that direct ozonation played a more important role than the indirect ozonation for degradation of *n*-alkanes. In addition, Fig. S8a shows that after 24 h of ozonation, 67.5% (by mass) of *n*-alkanes was degraded due to direct ozonation. Fig. 11c shows the volatilization, total ozonation and direct ozonation of PAHs under the same gas flow rate with or without *p*CBA. In the absence of *p*CBA, the ozonation rate constant of total PAHs was 0.048 h^{-1}; in the presence of *p*CBA, the ozonation rate constant was lowered to 0.022 h^{-1}, indicating that direct ozonation contributed 45.8% to the total ozonation of total PAHs. In addition, the parent and alkylated PAHs were degraded by 37.5% and 39.9% due to direct ozonation, respectively (Fig. S8b).

Ozone molecules can directly react with the C—H bonds in alkanes. The initial attack of ozone on alkanes is centered on the σ-bonding between C and H atoms, which includes 1,3-dipolar insertion, and subsequent transformation to isomers of ketones, racemized alcohols and peroxides, as illustrated by the following reactions (Hamilton et al., 1968):

$$RH + O_3 \rightarrow I \leftrightarrow II \quad (20)$$

$$I \rightarrow R\cdot + \cdot OH + O_2 \xrightarrow{O_2} ROH\,(racemized) + ketone + peroxides \quad (21)$$

$$I \text{ or } II \rightarrow ROH + O_2 \quad (22)$$

$$II \rightarrow ROOOH \rightarrow ROH + O_2 \quad (23)$$

where *I* and *II* are the transition states (or solvent caged intermediates) given by the initial attacking of alkanes by ozone (*I* is for [$R\cdot\ HO\cdot\ \cdot O{-}O\cdot$] and *II* is for [$R\cdot\ \cdot OOOH$]).

Direct reaction between PAHs and ozone lead to ring cleavage by electrophilic mechanisms (Bailey et al., 1968; Razumovskii, 2005), resulting in the formation of intermediates, such as quinones, hydroxylated and carboxylate benzenes, and oxygen derivatives of aliphatic compounds (Miller and Olejnik, 2004) (Eq. (24)). The intermediates may compete with the PAHs for both direct and indirect ozonation (Rubio-Clemente et al., 2014).

$$O_3 + PAH \rightarrow PAH_{ox} \rightarrow Intermediates \quad (24)$$

Ozonation of PAHs in DWAO solution can be attributed to several factors. On the one hand, the dispersant may promote the ozonation due to: 1) the dispersant-enhanced solubilization of molecular ozone can increase the formation of intermediates due to ring cleavage through direct oxidation and generation of free radicals (especially superoxide radicals), and 2) the ozone-facilitated alkylation not only promotes degradation of parent PAHs, but also leads to formation of more alkylated PAHs, which are known to be more ozone-reactive than the parent PAHs (Rubio-Clemente et al., 2014; von Gunten, 2003). On the other hand, the dispersant may inhibit the reaction due to: 1) the competition of intermediates with parent compounds for both molecular ozone and radicals, and 2) the competition of dispersant components, for instance, solvent propylene glycol can undergo both direct and indirect ozonolysis (Chou et al., 2006). The overall effect depends on the extent of these contrasting factors. In this work, the promoting effects for PAHs outran the inhibitive effects, and indirect ozonation attributed more than direct ozonation.

4. Conclusions

This study investigated the volatilization, direct ozonation and indirect ozonation of dispersed petroleum hydrocarbons in dispersant-oil-seawater systems under simulated atmospheric ozone. The primary findings are summarized as follows:

1) Corexit EC9500A accelerates ozonation of TPHs, *n*-alkanes and PAHs in DWAO. In the presence of 238 mg/L of Corexit EC9500A and at a gaseous ozone concentration of 86 ppbv, the pseudo first-order ozonation rate constants of TPHs, *n*-alkanes and total PAHs were 2.2, 1.01 and 1.96 times higher than those in WAO. Alkylated

Table 4
First-order ozonation rate constants for TPHs, *n*-alkanes and total PAHs in DWAO.

Type		Volatilization		Overall dissipation		Ozonation k_o (h^{-1}) k_R (h^{-1}) k_D (h^{-1})		
		k_v (h^{-1})	R^2	k (h^{-1})	R^2			
TPHs	Total ozonation	0.018	0.992	0.034	0.975	0.016	0.008	–
	Direct ozonation	0.018	0.992	0.026	0.999	0.009	–	0.009
n-alkanes	Total ozonation	0.009	0.999	0.051	0.984	0.042	0.033	
	Direct ozonation	0.009	0.999	0.026	0.956	0.018	–	0.018
Total PAHs	Total ozonation	0.015	0.964	0.063	0.966	0.048	0.026	
	Direct ozonation	0.015	0.964	0.036	0.956	0.022	–	0.022

PAHs were more prone to ozonation than parent PAHs in both WAO and DWAO.

2) Corexit EC9500A increased the concentrations of TPHs, *n*-alkanes and PAHs in DWAO by 189, 648 and 12 times, respectively, than in WAO. The dispersant is more effective for *n*-alkanes than PAHs.
3) The ozonation rates for all the oil compounds increased with increasing ozone concentration. The ozonation rates of TPHs, *n*-alkanes and total PAHs were increased by 14.8, 5.1 and 6.3 times when the gaseous ozone concentration was increased from 86 to 300 ppbv. PAHs, especially naphthalene and C1-phenanthrene, were more sensitive to the ozone concentration than *n*-alkanes in DWAO.
4) Increasing pH slightly inhibited ozonation, especially for the 2-, 3- and 4-ring PAHs and their homologs in DWAO due to the major loss in the direct ozonation. Elevated humic acid concentrations also inhibited the ozonation reactions, and the inhibitive effect of humic acid is more evident on larger *n*-alkanes, in particular the C24-C30 fraction. Higher salinity enhanced the ozonation of all the dispersed oil components due to reduced solvent cage effect and the salting-out effect of hydrophobic compounds. Meanwhile, addition of 18 mg/L or 24 mg/L of the dispersant to DWAO accelerated the ozonation of TPHs and *n*-alkanes, but inhibited the ozonation of PAHs due to ozone-facilitated alkylation process and dispersant cage effect.
5) Direct ozonation accounted for 56%, 54% and 45.8% of the overall ozonation of TPHs, *n*-alkanes and PAHs, respectively. For *n*-alkanes, the direct ozonation played a more important role. In contrast, for PAHs, the indirect ozonation was more important, respectively, especially for the 2-ring PAHs (naphthalene and its homologs, acenaphthylene and acenaphthene) and 3-ring PAHs (phenanthrene and its homologs). In addition, the parent and alkylated PAHs were degraded by 37.5% and 39.9% due to direct ozonation.
6) The dispersant can increase soluble ozone concentration and enhance the hydroxyl radical generation, but may also compete with oil hydrocarbons for both molecular ozone and free radicals. These contrasting effects result in the different reaction rates for various oil compounds.

This work is the first systematic investigation on oil weathering under simulated atmospheric ozone, and on the effects of a model oil dispersant on the ozonation rates of various oil components. The results indicate that ozonation may play an important role in oil weathering, and thus should be taken into account in the oil budget estimation and in the related impact assessment.

Acknowledgments

The research was partially supported by the U.S. Department of the Interior Bureau of Ocean Energy Management (M12AC00013), and the China Scholarship Council (201306930002).

Appendix A. Supplementary data

The following supplementary data are provided in the SM: Analytical methods for TPHs, PAHs and *n*-alkanes; Target PAHs and quantification ions (QIs); Chemical constituents of dispersant Corexit EC9500A; Pseudo first-order ozonation rate constants for parent and alkylated PAHs in WAO and DWAO; UV–Vis absorbance of aqueous ozone in DWAO; Volatilization and ozonation kinetic data of parent PAHs and alkylated PAHs in WAO and DWAO; Ozonation kinetics of parent PAHs and alkylated PAHs in DWAO under 86 ppbv simulated atmospheric ozone; Effect of pH on ozonation of parent and alkylated PAHs in DWAO by simulated atmospheric ozone; Distribution of remaining *n*-alkanes and PAHs in DWAO after 24 h ozonation at various levels of pH, humic acid, and salinity; Distribution of remaining *n*-alkanes and PAHs after 24 h of ozonation (overall versus direct ozonation). Supplementary data to this article can be found online at doi:https://doi.org/10.1016/j.marpolbul.2018.07.047.

References

ADEM, 2016. Alabama 8-hour ozone data. http://www.adem.state.al.us/programs/air/airquality/ozone/8HourOzoneData.pdf, Accessed date: 8 September 2016.
Bacosa, H.P., Erdner, D.L., Liu, Z.F., 2015. Differentiating the roles of photooxidation and biodegradation in the weathering of light Louisiana sweet crude oil in surface water from the Deepwater Horizon site. Mar. Pollut. Bull. 95, 265–272.
Bader, H., Hoigné, J., 1981. Determination of ozone in water by the indigo method. Water Res. 15, 449–456.
Bailey, P.S., Batterbee, J.E., Lane, A.G., 1968. Ozonation of benz[*a*]anthracene. J. Am. Chem. Soc. 90, 1027–1033.
Baumard, P., Budzinski, H., Garrigues, P., Sorbe, J.C., Burgeot, T., Bellocq, J., 1998. Concentrations of PAHs (polycyclic aromatic hydrocarbons) in various marine organisms in relation to those in sediments and to trophic level. Mar. Pollut. Bull. 36, 951–960.
Beltran, F.J., Ovejero, G., Encinar, J.M., Rivas, J., 1995. Oxidation of polynuclear aromatic hydrocarbons in water. 1. Ozonation. Ind. Eng. Chem. Rev. 34, 1596–1606.
Board M, Council N.R, 1989. Using Oil Spill Dispersants on the Sea. National Academies Press.
Cai, Z., Gong, Y., Liu, W., Fu, J., O'Reilly, S.E., Hao, X., et al., 2016. A surface tension based method for measuring oil dispersant concentration in seawater. Mar. Pollut. Bull. 109, 49–54.
Camilli, R., Reddy, C.M., Yoerger, D.R., Van Mooy, B., Jakuba, M.V., Kinsey, J.C., et al., 2010. Tracking hydrocarbon plume transport and biodegradation at Deepwater Horizon. Science 330, 201–204.
Chelme-Ayala, P., El-Din, M.G., Smith, D.W., Adams, C.D., 2011. Oxidation kinetics of two pesticides in natural waters by ozonation and ozone combined with hydrogen peroxide. Water Res. 45, 2517–2526.
Chiu, C., Chen, Y., Huang, Y., 2007. Removal of naphthalene in Brij 30-containing solution by ozonation using rotating packed bed. J. Hazard. Mater. 147, 732–737.
Chou, M., Huang, B., Chang, H., 2006. Degradation of gas-phase propylene glycol monomethyl ether acetate by ultraviolet/ozone process: a kinetic study. J. Air Waste Manage. Assoc. 56, 767–776.
Chu, W., Chan, K.H., Graham, N.J.D., 2006. Enhancement of ozone oxidation and its associated processes in the presence of surfactant: degradation of atrazine. Chemosphere 64, 931–936.
Conmy, R.N., Coble, P.G., Farr, J., Wood, A.M., Lee, K., Pegau, W.S., et al., 2014. Submersible optical sensors exposed to chemically dispersed crude oil: wave tank simulations for improved oil spill monitoring. Environ. Sci. Technol. 48, 1803–1810.
Couillard, C.M., Lee, K., Légaré, B., King, T.L., 2005. Effect of dispersant on the composition of the water-accommodated fraction of crude oil and its toxicity to larval marine fish. Environ. Toxicol. Chem. 24, 1496–1504.
Diallo, M.S., Abriola, L.M., Weber, W.J., 1994. Solubilization of nonaqueous phase liquid hydrocarbons in micellar solutions of dodecyl alcohol ethoxylates. Environ. Sci. Technol. 28, 1829–1837.
Elovitz, M.S., von Gunten, U., 1999. Hydroxyl radical/ozone ratios during ozonation processes. I. The R_{ct} concept. Ozone Sci. Eng. 21, 239–260.
Elovitz, M.S., von Gunten, U., Kaiser, H.P., 2000. Hydroxyl radical/ozone ratios during ozonation processes. II. The effect of temperature, pH, alkalinity, and DOM

properties. Ozone Sci. Eng. 22, 123–150.
EPA, 1984. EPA method 610. https://www.epa.gov/sites/production/files/2015-10/documents/method_610_1984.pdf, Accessed date: October 2015.
EPA, 1996. EPA 3510C. https://www.epa.gov/sites/production/files/2015-12/documents/3510c.pdf, Accessed date: December 2015.
EPA, 2017. Outdoor Air Quality Data. Monitor Values Report. https://www.epa.gov/outdoor-air-quality-data/monitor-values-report.
Eriksson, M., 2005. Ozone Chemistry in Aqueous Solution: Ozone Decomposition and Stabilization (PhD diss.). KTH.
Forni, L., Bahnemann, D., Hart, E.J., 1982. Mechanism of the hydroxide ion-initiated decomposition of ozone in aqueous solution. J. Phys. Chem. 86, 255–259.
Fu, J., Gong, Y., Zhao, X., O'Reilly, S.E., Zhao, D., 2014. Effects of oil and dispersant on formation of marine oil snow and transport of oil hydrocarbons. Environ. Sci. Technol. 48, 14392–14399.
Fu, J., Gong, Y., Cai, Z., O'Reilly, S.E., Zhao, D., 2017. Mechanistic investigation into sunlight-facilitated photodegradation of pyrene in seawater with oil dispersants. Mar. Pollut. Bull. 114, 751–758.
Fujita, H., Izumi, J., Sagehashi, M., Fujii, T., Sakoda, A., 2004. Adsorption and decomposition of water-dissolved ozone on high silica zeolites. Water Res. 38, 159–165.
Gong, Y., Zhao, D., 2017. Effects of oil dispersant on ozone oxidation of phenanthrene and pyrene in marine water. Chemosphere 172, 468–475.
Gong, Y., Zhao, X., O'Reilly, S.E., Qian, T., Zhao, D., 2014. Effects of oil dispersant and oil on sorption and desorption of phenanthrene with Gulf Coast marine sediments. Environ. Pollut. 185, 240–249.
Gong, Y., Fu, J., O'Reilly, S.E., Zhao, D., 2015. Effects of oil dispersants on photodegradation of pyrene in marine water. J. Hazard. Mater. 287, 142–150.
Haagen-Smit, A.J., Bradley, C.E., Fox, M.M., 1953. Ozone formation in photochemical oxidation of organic substances. Ind. Eng. Chem. 45 (9), 2086–2089.
Hamilton, G.A., Ribner, B.S., Hellman, T.M., 1968. The mechanism of alkane oxidation by ozone. Adv. Chem. 77.
Hellman, T.M., Hamilton, G.A., 1974. Mechanism of alkane oxidation by ozone in the presence and absence of iron (III) chloride. J. Am. Chem. Soc. 96, 1530–1535.
Hemmer, M.J., Barron, M.G., Greene, R.M., 2011. Comparative toxicity of eight oil dispersants, Louisiana sweet crude oil (LSC), and chemically dispersed LSC to two aquatic test species. Environ. Toxicol. Chem. 30, 2244–2252.
Kasprzyk-Hordern, B., Ziolek, M., Nawrocki, J., 2003. Catalytic ozonation and methods of enhancing molecular ozone reactions in water treatment. Appl. Catal. B 46, 639–669.
Kleindienst, S., Paul, J.H., Joye, S.B., 2015. Using dispersants after oil spills: impacts on the composition and activity of microbial communities. Nat. Rev. Microbiol. 13, 388.
Kujawinski, E.B., Kido Soule, M.C., Valentine, D.L., Boysen, A.K., Longnecker, K., Redmond, M.C., 2011. Fate of dispersants associated with the Deepwater Horizon oil spill. Environ. Sci. Technol. 45, 1298–1306.
Li, Z., Lee, K., King, T., Boufadel, M.C., Venosa, A.D., 2009. Evaluating chemical dispersant efficacy in an experimental wave tank: 2—significant factors determining in situ oil droplet size distribution. Environ. Eng. Sci. 26, 1407–1418.
Lima, A.L., Farrington, J.W., Reddy, C.M., 2005. Combustion-derived polycyclic aromatic hydrocarbons in the environment—a review. Environ. Forensic 6 (2), 109–131.
Lin, C., Zhang, W., Yuan, M., Feng, C., Ren, Y., Wei, C., 2014. Degradation of polycyclic aromatic hydrocarbons in a coking wastewater treatment plant residual by an O_3/ultraviolet fluidized bed reactor. Environ. Sci. Pollut. Res. 21, 10329–10338.
Litter, M., Quici, N., 2010. Photochemical advanced oxidation processes for water and wastewater treatment. Recent Patents Eng. 4, 217–241.
Liu, Z., Liu, J., Zhu, Q., Wu, W., 2012. The weathering of oil after the Deepwater Horizon oil spill: insights from the chemical composition of the oil from the sea surface, salt marshes and sediments. Environ. Res. Lett. 7, 035302.
Liu, Z., Liu, J., Gardner, W.S., Shank, G.C., Ostrom, N.E., 2016. The impact of Deepwater Horizon oil spill on petroleum hydrocarbons in surface waters of the northern Gulf of Mexico. Deep-Sea Res. II Top. Stud. Oceanogr. 129, 292–300.
Liu, J., Bacosa, H.P., Liu, Z., 2017. Potential environmental factors affecting oil-degrading bacterial populations in deep and surface waters of the northern Gulf of Mexico. Front. Microbiol. 10 (7), 2131.
Masten, S.J., Davies, S.H., 1994. The use of ozonation to degrade organic contaminants in wastewaters. Environ. Sci. Technol. 28, 180A–185A.
Miller, J.S., Olejnik, D., 2004. Ozonation of polycyclic aromatic hydrocarbons in water solution. Ozone Sci. Eng. 26, 453–464.
Muthukumar, M., Selvakumar, N., 2004. Studies on the effect of inorganic salts on decolouration of acid dye effluents by ozonation. Dyes Pigments 62, 221–228.
Ning, X., Shen, L., Sun, J., Lin, C., Zhang, Y., Yang, Z., et al., 2015. Degradation of polycyclic aromatic hydrocarbons (PAHs) in textile dyeing sludge by O_3/H_2O_2 treatment. RSC Adv. 5, 38021–38029.
Place, B., Anderson, B., Mekebri, A., Furlong, E.T., Gray, J.L., Tjeerdema, R., et al., 2010. A role for analytical chemistry in advancing our understanding of the occurrence, fate, and effects of Corexit oil dispersants. Environ. Sci. Technol. 44, 6016–6018.
Pryor, W.A., Wu, M., 1992. Ozonation of methyl oleate in hexane, in a thin film, in SDS micelles, and in distearoylphosphatidylcholine liposomes: yields and properties of the Criegee ozonide. Chem. Rev. Toxicol. 5, 505–511.
Ramseur, J.L., 2010. Deepwater Horizon oil spill: the fate of the oil. In: Congressional Research Service. Library of Congress, Washington, DC.
Razumovskii, S., 2005. Reactions of ozone with aromatic compounds. Chem. Kinet. 259.
Reddy, C.M., Arey, J.S., Seewald, J.S., Sylva, S.P., Lemkau, K.L., Nelson, R.K., et al., 2012. Composition and fate of gas and oil released to the water column during the Deepwater Horizon oil spill. Proc. Natl. Acad. Sci. 109, 20229–20234.
Ringuet, J., Albinet, A., Leoz-Garziandia, E., Budzinski, H., Villenave, E., 2012. Reactivity of polycyclic aromatic compounds (PAHs, NPAHs and OPAHs) adsorbed on natural aerosol particles exposed to atmospheric oxidants. Atmos. Environ. 61, 15–22.
Rosenfeldt, E.J., Linden, K.G., Canonica, S., von Gunten, U., 2006. Comparison of the efficiency of OH radical formation during ozonation and the advanced oxidation processes O_3/H_2O_2 and UV/H_2O_2. Water Res. 40, 3695–3704.
Rubio-Clemente, A., Torres-Palma, R.A., Peñuela, G.A., 2014. Removal of polycyclic aromatic hydrocarbons in aqueous environment by chemical treatments: a review. Sci. Total Environ. 478, 201–225.
Ryerson, T.B., Aikin, K.C., Angevine, W.M., Atlas, E.L., Blake, D.R., Brock, C.A., et al., 2011. Atmospheric emissions from the Deepwater Horizon spill constrain air-water partitioning, hydrocarbon fate, and leak rate. Geophys. Res. Lett. 38, L07803.
Sammarco, P.W., Kolian, S.R., Warby, R.A., Bouldin, J.L., Subra, W.A., Porter, S.A., 2013. Distribution and concentrations of petroleum hydrocarbons associated with the BP/Deepwater Horizon oil spill, Gulf of Mexico. Mar. Pollut. Bull. 73, 129–143.
Scelfo, G.M., Tjeerdema, R.S., 1991. A simple method for determination of Corexit 9527® in natural waters. Mar. Environ. Res. 31, 69–78.
Simpson, M.J., Simpson, A.J., Hatcher, P.G., 2004. Noncovalent interactions between aromatic compounds and dissolved humic acid examined by nuclear magnetic resonance spectroscopy. Environ. Toxicol. Chem. 23, 355–362.
Singer, M.M., Aurand, D., Bragin, G.E., Clark, J.R., Coelho, G.M., Sowby, M.L., et al., 2000. Standardization of the preparation and quantitation of water-accommodated fractions of petroleum for toxicity testing. Mar. Pollut. Bull. 40, 1007–1016.
Sorial, G., Chandrasekar, S., Weaver, J.W., 2004. Characteristics of Spilled Oils, Fuels, and Petroleum Products: 2a. Dispersant Effectiveness Data for a Suite of Environmental Conditions–The Effects of Temperature, Volatilization, and Energy. EPA/600/R-04/119. http://www.epa.gov/athens/research/projects/eros, Accessed date: 8 September 2004.
Staehelin, J., Hoigne, J., 1985. Decomposition of ozone in water in the presence of organic solutes acting as promoters and inhibitors of radical chain reactions. Environ. Sci. Technol. 19, 1206–1213.
Vikhorev, A.A., Syroezhko, A.M., Proskuryakov, V.A., Yakovlev, A.S., 1978. Oxidation of Normal Decane by Ozone-Air Mixtures. J. Appl. Chem. USSR 51, 2448–2451.
von Gunten, U., 2003. Ozonation of drinking water: part I. Oxidation kinetics and product formation. Water Res. 37, 1443–1467.
Walter, T., Ederer, H., Först, C., Stieglitz, L., 2000. Sorption of selected polycyclic aromatic hydrocarbons on soils in oil-contaminated systems. Chemosphere 41, 387–397.
Yin, F., John, G.F., Hayworth, J.S., Clement, T.P., 2015. Long-term monitoring data to describe the fate of polycyclic aromatic hydrocarbons in Deepwater Horizon oil submerged off Alabama's beaches. Sci. Total Environ. 508, 46–56.
Yu, D.Y., Kang, N., Bae, W., Banks, M.K., 2007. Characteristics in oxidative degradation by ozone for saturated hydrocarbons in soil contaminated with diesel fuel. Chemosphere 66, 799–807.
Zhang, Y., Wong, J., Liu, P., Yuan, M., 2011. Heterogeneous photocatalytic degradation of phenanthrene in surfactant solution containing TiO_2 particles. J. Hazard. Mater. 191, 136–143.
Zhang, Y., Zhou, L., Zeng, C., Wang, Q., Wang, Z., Gao, S., et al., 2013. Photoreactivity of hydroxylated multi-walled carbon nanotubes and its effects on the photodegradation of atenolol in water. Chemosphere 93, 1747–1754.
Zhao, W., Shi, H., Wang, D., 2004. Ozonation of cationic red X-GRL in aqueous solution: degradation and mechanism. Chemosphere 57, 1189–1199.
Zhao, W., Liu, F., Yang, Y., Tan, M., Zhao, D., 2011. Ozonation of cationic red X-GRL in aqueous solution: kinetics and modeling. J. Hazard. Mater. 187, 526–533.
Zhao, X., Gong, Y., O'Reilly, S.E., Zhao, D., 2015. Effects of oil dispersant on solubilization, sorption and desorption of polycyclic aromatic hydrocarbons in sediment–seawater systems. Mar. Pollut. Bull. 92, 160–169.
Zhao, X., Liu, W., Fu, J., Cai, Z., O'Reilly, S.E., Zhao, D., 2016. Dispersion, sorption and photodegradation of petroleum hydrocarbons in dispersant-seawater-sediment systems. Mar. Pollut. Bull. 109, 526–538.